(Hyper)tension release by N-terminal acetylation

Henriette Aksnes[1], Adrian Drazic[1], and Thomas Arnesen[1,2]

[1] Department of Molecular Biology, University of Bergen, N-5020 Bergen, Norway
[2] Department of Surgery, Haukeland University Hospital, N-5021 Bergen, Norway

A recent study links N-terminal acetylation and N-end rule degradation to blood pressure regulation. N-terminal mutants of Rgs2, a key G-protein regulator, are differentially processed by N-terminal acetyltransferases and the two branches of the N-end rule pathway. This leads to an imbalance in the signaling governing blood pressure.

Glossary

Hypertension: high blood pressure and major risk factor for cardiovascular diseases.

N-terminal (Nt) acetylation: common protein modification (occurring on ~80% of proteins) that involves the conjugation of an acetyl group (-COCH$_3$) to the N terminus of a protein (Nt-acetylation occurs largely co-translationally).
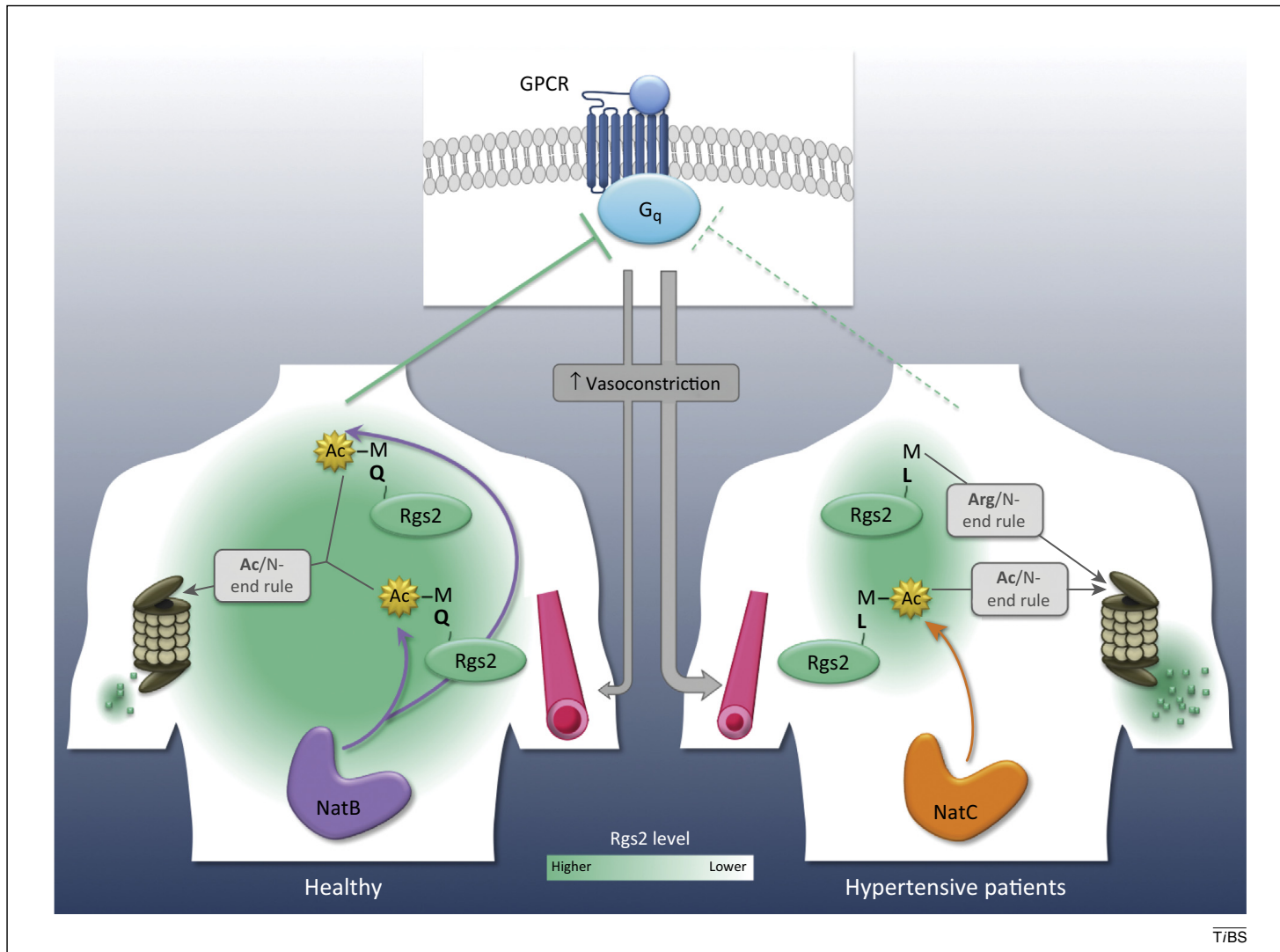
N-terminal acetyltransferases (NATs): substrate-specific enzymes that catalyze N-terminal acetylation.

N-end rule pathway: a ubiquitin/proteasome-dependent proteolytic system that recognizes degradation signals (degrons) whose main determinant is a destabilizing N-terminal residue. It consists of two distinguished branches, the Ac/N-end rule and the Arg/N-end rule pathway. The Ac/N-end rule branch targets proteins with specific residues that are N-terminally acetylated. The Arg/N-end rule branch instead targets proteins with unacetylated, destabilizing N-terminal residues.

N-degron: an N-terminal degradation signal recognized by the N-end rule pathway. Ac/N-degrons specifically include an acetylated N-terminal residue (e.g., Ac-Met, Ac-Ala, Ac-Ser, Ac-Thr, and sometimes Ac-Val and Ac-Cys). Arg/N-degrons have Arg, Lys, His, Leu, Phe, Tyr, Trp, or Ile, or unacetylated Met when followed by a non-Met hydrophobic residue (Met-Φ/N-degron).

N-recognin: a ubiquitin ligase that recognizes N-degrons.

Vasoconstriction: the constriction of blood vessels, which increases blood pressure.
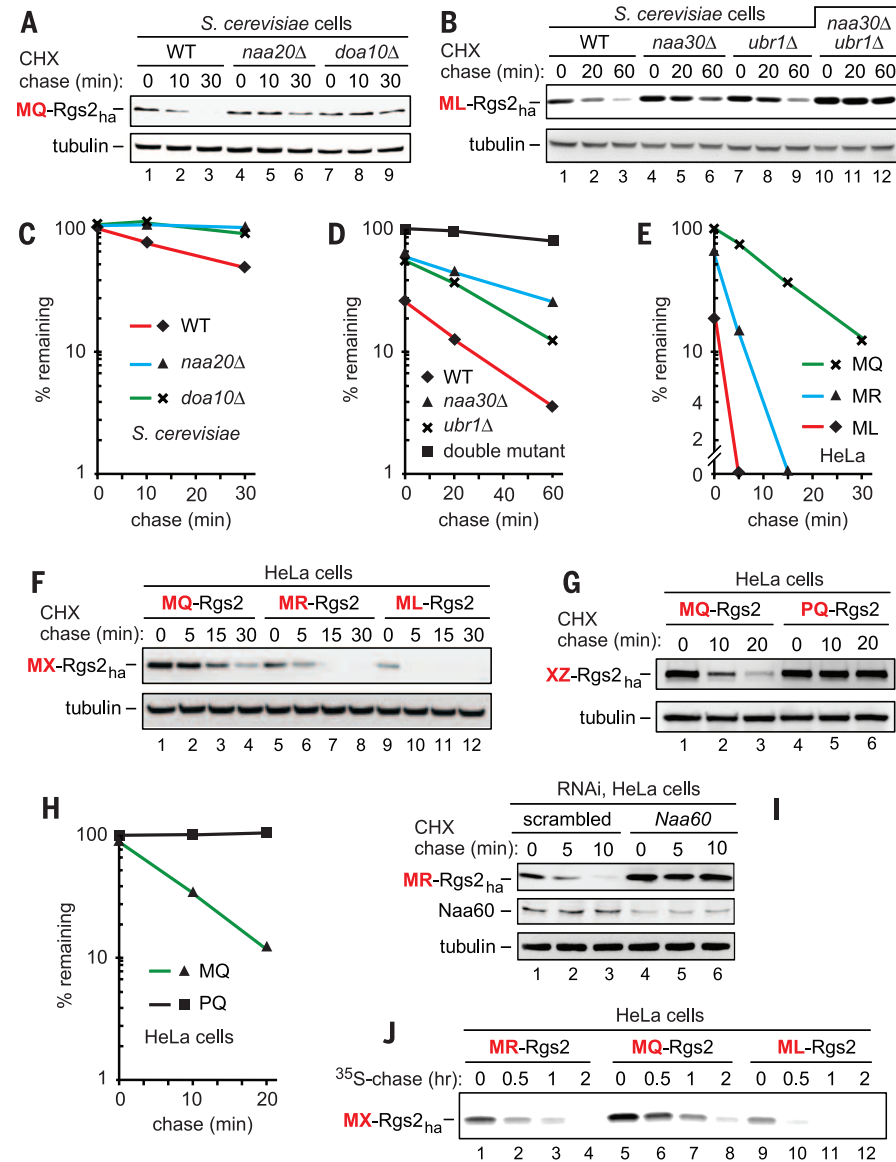
Figure 1. **N-terminal acetylation and the N-end rule pathway regulate Gq signaling and thereby hypertension.** Regulator of G-protein signaling 2 (Rgs2, green), is a key protein in the regulation of blood pressure through its inhibition of Gq protein signaling, which increases vasoconstriction and hence blood pressure. In healthy individuals (left), wild-type Rgs2 (MQ-Rgs2) is subjected to N-terminal acetylation by the NatB Nt-acetyltransferase (purple), followed by degradation via the Ac/N-end rule pathway. The ML-Rgs2 mutant is associated with hypertension in human patients (right). Although this mutant cannot be Nt-acetylated by NatB (in contrast to wild-type MQ-Rgs2), it can be Nt-acetylated by NatC (orange). This change is likely to result in, among other things, a partial Nt-acetylation of ML-Rgs2. The pool of unacetylated ML-Rgs2 molecules is targeted by the Arg/N-end rule pathway, which recognizes the unacetylated Met residue if another hydrophobic residue follows it [7]. The pool of Nt-acetylated ML-Rgs2 is targeted by the Ac/N-end rule pathway, similar to wild-type MQ-Rgs2. This dual degradation of mutant ML-Rgs2 by two different branches of the N-end rule pathway strongly downregulates ML-Rgs2 and thereby increases the activity of G-protein signaling pathways that are normally repressed by Rgs2, resulting in excessive vasoconstriction. The levels of another hypertension-associated variant, MR-Rgs2 (not shown), were also found to be lower than those of wild-type MQ-Rgs2, in the order MQ > MR > ML [6]. MR-Rgs2 was analyzed less extensively and the reasons for its decreased cellular levels remain to be fully understood. Nevertheless, the decreased cellular levels of both ML-Rgs2 and MR-Rgs2 are likely to account for the hypertension phenotypes conferred by these mutations in human Rgs2.

Control of mammalian G protein signaling by N-terminal acetylation and the N-end rule pathway

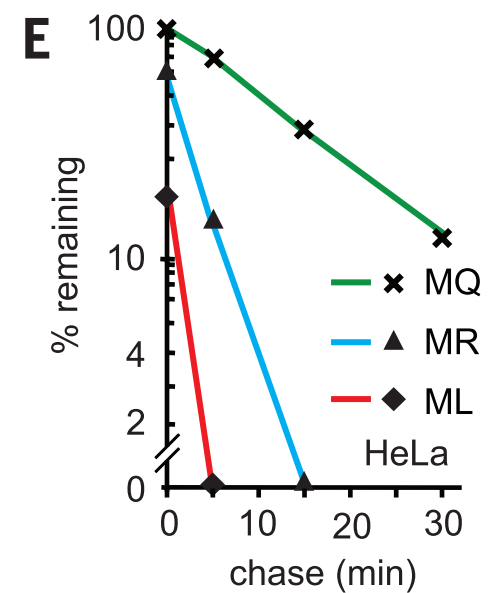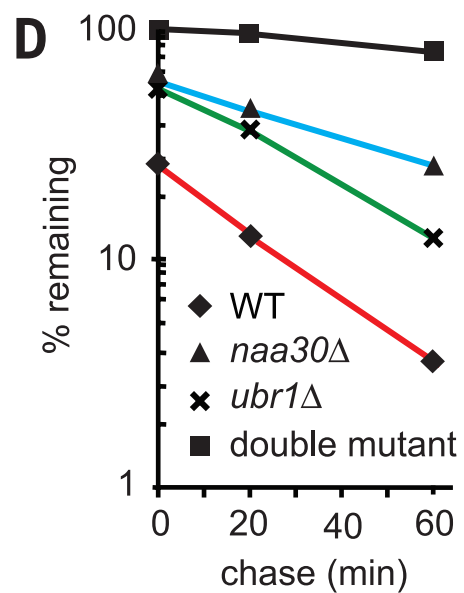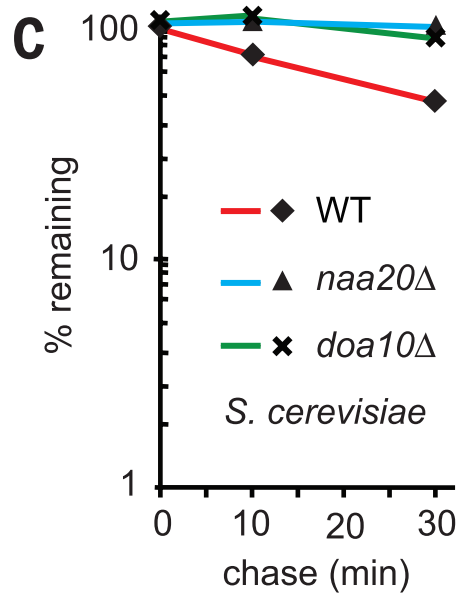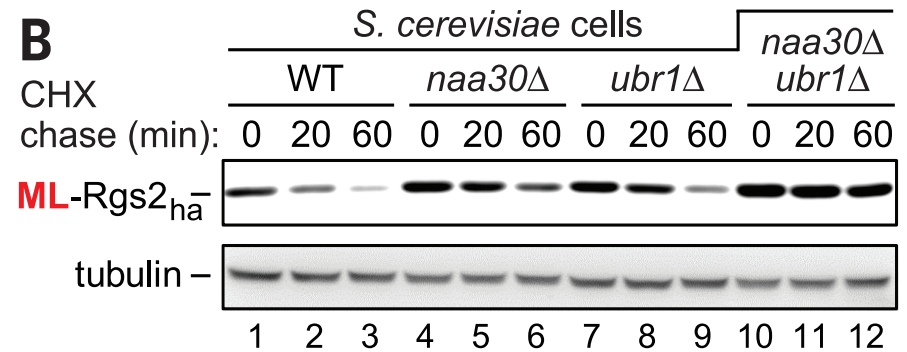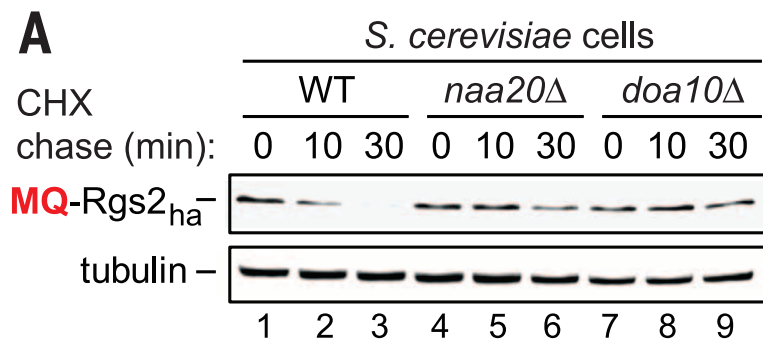Sang-Eun Park,[1]* Jeong-Mok Kim,[1]* Ok-Hee Seok,[1] Hanna Cho,[1] Brandon Wadas,[2] Seon-Young Kim,[3,4] Alexander Varshavsky,[2]† Cheol-Sang Hwang[1]†
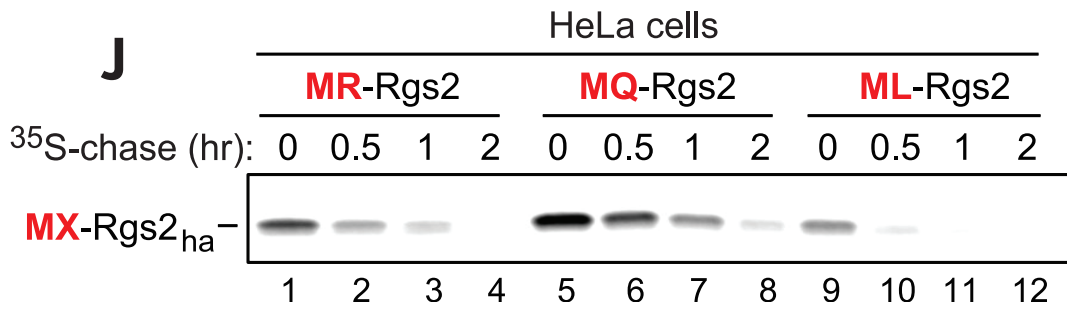
Rgs2, a regulator of G proteins, lowers blood pressure by decreasing signaling through $G\alpha_q$. Human patients expressing Met-Leu-Rgs2 (ML-Rgs2) or Met-Arg-Rgs2 (MR-Rgs2) are hypertensive relative to people expressing wild-type Met-Gln-Rgs2 (MQ-Rgs2). We found that wild-type MQ-Rgs2 and its mutant, MR-Rgs2, were destroyed by the Ac/N-end rule pathway, which recognizes N^α-terminally acetylated (Nt-acetylated) proteins. The shortest-lived mutant, ML-Rgs2, was targeted by both the Ac/N-end rule and Arg/N-end rule pathways. The latter pathway recognizes unacetylated N-terminal residues. Thus, the Nt-acetylated Ac-MX-Rgs2 (X = Arg, Gln, Leu) proteins are specific substrates of the mammalian Ac/N-end rule pathway. Furthermore, the Ac/N-degron of Ac-MQ-Rgs2 was conditional, and Teb4, an endoplasmic reticulum (ER) membrane-embedded ubiquitin ligase, was able to regulate G protein signaling by targeting Ac-MX-Rgs2 proteins for degradation through their N^α-terminal acetyl group.

Fig. 1. Rgs2 as an N-end rule substrate. (**A**) CHX chases with wild-type human MQ-Rgs2$_{ha}$ in wild-type, naa20Δ, and doa10Δ S. cerevisiae. (**B**) As in (A) but with ML-Rgs2$_{ha}$ in wild-type, naa30Δ, ubr1Δ, and naa30Δ ubr1Δ strains. (**C** to **E**) Quantification of data in (A), (B), and (F), respectively. See the legend to fig. S3 for definitions of "100%" levels at zero time. (**F**) CHX chases with exogenously expressed MX-Rgs2$_{ha}$ (X = Arg, Gln, Leu) in HeLa cells. (**G**) As in (F) but with MQ-Rgs2$_{ha}$ versus PQ-Rgs2$_{ha}$. (**H**) Quantification of data in (G). (**I**) CHX chases with exogenously expressed MR-Rgs2 in HeLa cells subjected to RNAi for a either a "scrambled" target or Naa60. (**J**) ^{35}S-pulse chases with MX-Rgs2$_{ha}$ (X = Arg, Gln, Leu) in HeLa cells.

Fig. 1. Rgs2 as an N-end rule substrate. (**A**) CHX chases with wild-type human MQ-Rgs2$_{ha}$ in wild-type, *naa20Δ*, and *doa10Δ S. cerevisiae*. (**B**) As in (A) but with ML-Rgs2$_{ha}$ in wild-type, *naa30Δ*, *ubr1Δ*, and *naa30Δ ubr1Δ* strains. (**C** to **E**) Quantification of data in (A), (B), and (F), respectively. See the legend to fig. S3 for definitions of "100%" levels at zero time. (**F**) CHX chases with exogenously expressed MX-Rgs2$_{ha}$ (X = Arg, Gln, Leu) in HeLa cells. (**G**) As in (F) but with MQ-Rgs2$_{ha}$ versus PQ-Rgs2$_{ha}$. (**H**) Quantification of data in (G). (**I**) CHX chases with exogenously expressed MR-Rgs2 in HeLa cells subjected to RNAi for a either a "scrambled" target or Naa60. (**J**) ^{35}S-pulse chases with MX-Rgs2$_{ha}$ (X = Arg, Gln, Leu) in HeLa cells.

A

S. cerevisiae cells

CHX chase (min): WT 0 10 30 | *naa20Δ* 0 10 30 | *doa10Δ* 0 10 30

MQ-Rgs2ha−

tubulin −

1 2 3 4 5 6 7 8 9

B

S. cerevisiae cells | *naa30Δ ubr1Δ*

CHX chase (min): WT 0 20 60 | *naa30Δ* 0 20 60 | *ubr1Δ* 0 20 60 | 0 20 60

ML-Rgs2ha−

tubulin −

1 2 3 4 5 6 7 8 9 10 11 12

C

% remaining

WT
naa20Δ
doa10Δ

S. cerevisiae

chase (min)

D

% remaining

WT
naa30Δ
ubr1Δ
double mutant

chase (min)

E

% remaining

MQ
MR
ML

HeLa

chase (min)

F

HeLa cells

CHX chase (min): **MQ**-Rgs2 | **MR**-Rgs2 | **ML**-Rgs2
0 5 15 30 | 0 5 15 30 | 0 5 15 30

MX-Rgs2$_{ha}$—

tubulin—

1 2 3 4 5 6 7 8 9 10 11 12

G

HeLa cells

CHX chase (min): **MQ**-Rgs2 | **PQ**-Rgs2
0 10 20 | 0 10 20

XZ-Rgs2$_{ha}$—

tubulin—

1 2 3 4 5 6

H

% remaining vs chase (min)

— ▲ MQ
— ■ PQ

HeLa cells

I

RNAi, HeLa cells

CHX chase (min): scrambled | *Naa60*
0 5 10 | 0 5 10

MR-Rgs2$_{ha}$—

Naa60 —

tubulin —

1 2 3 4 5 6

J

HeLa cells

^{35}S-chase (hr): **MR**-Rgs2 | **MQ**-Rgs2 | **ML**-Rgs2
0 0.5 1 2 | 0 0.5 1 2 | 0 0.5 1 2

MX-Rgs2$_{ha}$—

1 2 3 4 5 6 7 8 9 10 11 12

Fig. 2. Teb4 as an Ac/N-recognin. (**A**) MQ-Rgs2$_{ha}$ in HeLa cells with or without Teb4$_{3f}$ or the MG132 proteasome inhibitor. (**B**) CHX chases with endogenous MQ-Rgs2, Teb4, and Naa20 subjected to RNAi for a "scrambled" target, Teb4, or Naa20. The asterisk indicates a protein cross-reacting with anti-Teb4. (**C**) Molecular weight standards, purified MQ-Rgs2$^{1-10}$-GST, and purified Ac-MQ-Rgs2$^{1-10}$-GST, respectively. (**D**) Lane 1, Teb4$_{3f}$ input; lanes 2 to 4, GST pull-downs with GST alone, MQ-Rgs2$^{1-10}$-GST, and Ac-MQ-Rgs2$^{1-10}$-GST, respectively. (**E**) As in (D) but Coomassie-stained GST fusions released from beads. (**F**) MQ-Rgs2$_{ha}$ in HeLa cells overexpressing wild-type Teb4$_{3f}$ or Teb4$_{3f}^{C9A}$. (**G**) Increases in Teb4$_{3f}$ led to decreases in MQ-Rgs2$_{ha}$. (**H**) HeLa cells expressing MQ-Rgs2$_{ha}$ alone (lane 1) or together with Teb4$_{3f}$ (lane 2) were treated with a cell-penetrating cross-linker, followed by immunoprecipitations with anti-FLAG, reversal of cross-links, SDS–polyacrylamide gel electrophoresis (PAGE), and immunoblotting with anti-HA and anti-FLAG. (**I**) As in (H) but Teb4$_{3f}$ alone in lane 1, and immunoprecipitations with anti-HA.
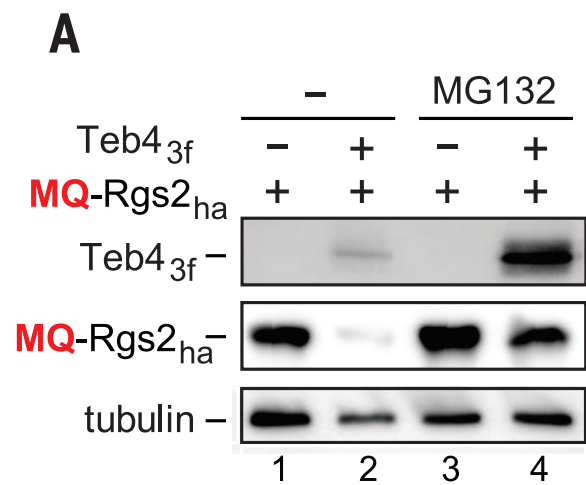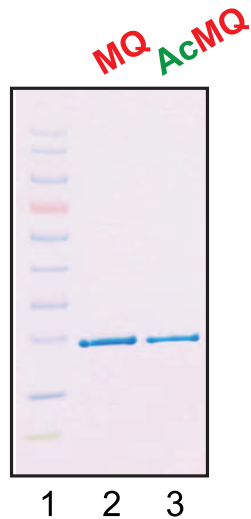
Fig. 2. Teb4 as an Ac/N-recognin. (**A**) MQ-Rgs2$_{ha}$ in HeLa cells with or without Teb4$_{3f}$ or the MG132 proteasome inhibitor. (**B**) CHX chases with endogenous MQ-Rgs2, Teb4, and Naa20 subjected to RNAi for a "scrambled" target, Teb4, or Naa20. The asterisk indicates a protein cross-reacting with anti-Teb4. (**C**) Molecular weight standards, purified MQ-Rgs2$^{1\text{-}10}$-GST, and purified Ac-MQ-Rgs2$^{1\text{-}10}$-GST, respectively. (**D**) Lane 1, Teb4$_{3f}$ input; lanes 2 to 4, GST pull-downs with GST alone, MQ-Rgs2$^{1\text{-}10}$-GST, and Ac-MQ-Rgs2$^{1\text{-}10}$-GST, respectively. (**E**) As in (D) but Coomassie-stained GST fusions released from beads. (**F**) MQ-Rgs2$_{ha}$ in HeLa cells overexpressing wild-type Teb4$_{3f}$ or Teb4$_{3f}^{C9A}$. (**G**) Increases in Teb4$_{3f}$ led to decreases in MQ-Rgs2$_{ha}$. (**H**) HeLa cells expressing MQ-Rgs2$_{ha}$ alone (lane 1) or together with Teb4$_{3f}$ (lane 2) were treated with a cell-penetrating cross-linker, followed by immunoprecipitations with anti-FLAG, reversal of cross-links, SDS–polyacrylamide gel electrophoresis (PAGE), and immunoblotting with anti-HA and anti-FLAG. (**I**) As in (H) but Teb4$_{3f}$ alone in lane 1, and immunoprecipitations with anti-HA.
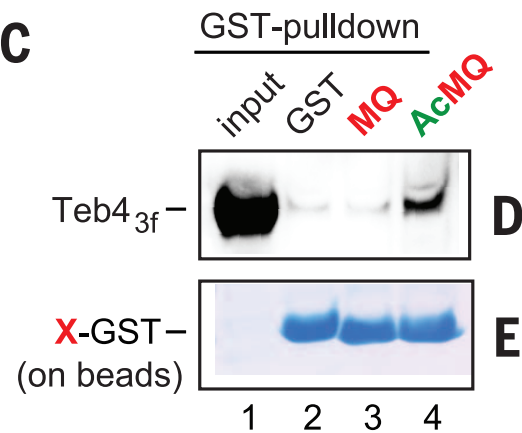
A

MG132

Teb4 3f   −   +   −   +
MQ-Rgs2 ha   +   +   +   +

Teb4 3f −

MQ-Rgs2 ha −

tubulin −

1   2   3   4

B   RNAi, HeLa cells

scrambled   *Teb4*   *Naa20*

CHX
chase (hr):   0   4   8   0   4   8   0   4   8

MQ-Rgs2 −
(endogenous)

tubulin −

Teb4 * −
(endogenous)

Naa20 −
(endogenous)

1   2   3   4   5   6   7   8   9

MQ-Rgs2$^{1-10}$-[GST]

MQ   AcMQ

1   2   3

C   GST-pulldown

input   GST   MQ   AcMQ

Teb4 3f −   **D**

X-GST −   **E**
(on beads)

1   2   3   4

F   active vs. inactive Teb4

wt Teb4 3f   −   −   +
Teb4$_{3f}^{C9A}$ −   +   −

Teb4 3f −

MQ-Rgs2 ha −

tubulin −

1   2   3

Fig. 2. Teb4 as an Ac/N-recognin. (**A**) MQ-Rgs2$_{ha}$ in HeLa cells with or without Teb4$_{3f}$ or the MG132 proteasome inhibitor. (**B**) CHX chases with endogenous MQ-Rgs2, Teb4, and Naa20 subjected to RNAi for a "scrambled" target, Teb4, or Naa20. The asterisk indicates a protein cross-reacting with anti-Teb4. (**C**) Molecular weight standards, purified MQ-Rgs2$^{1\text{-}10}$-GST, and purified Ac-MQ-Rgs2$^{1\text{-}10}$-GST, respectively. (**D**) Lane 1, Teb4$_{3f}$ input; lanes 2 to 4, GST pull-downs with GST alone, MQ-Rgs2$^{1\text{-}10}$-GST, and Ac-MQ-Rgs2$^{1\text{-}10}$-GST, respectively. (**E**) As in (D) but Coomassie-stained GST fusions released from beads. (**F**) MQ-Rgs2$_{ha}$ in HeLa cells overexpressing wild-type Teb4$_{3f}$ or Teb4$_{3f}^{C9A}$. (**G**) Increases in Teb4$_{3f}$ led to decreases in MQ-Rgs2$_{ha}$. (**H**) HeLa cells expressing MQ-Rgs2$_{ha}$ alone (lane 1) or together with Teb4$_{3f}$ (lane 2) were treated with a cell-penetrating cross-linker, followed by immunoprecipitations with anti-FLAG, reversal of cross-links, SDS–polyacrylamide gel electrophoresis (PAGE), and immunoblotting with anti-HA and anti-FLAG. (**I**) As in (H) but Teb4$_{3f}$ alone in lane 1, and immunoprecipitations with anti-HA.
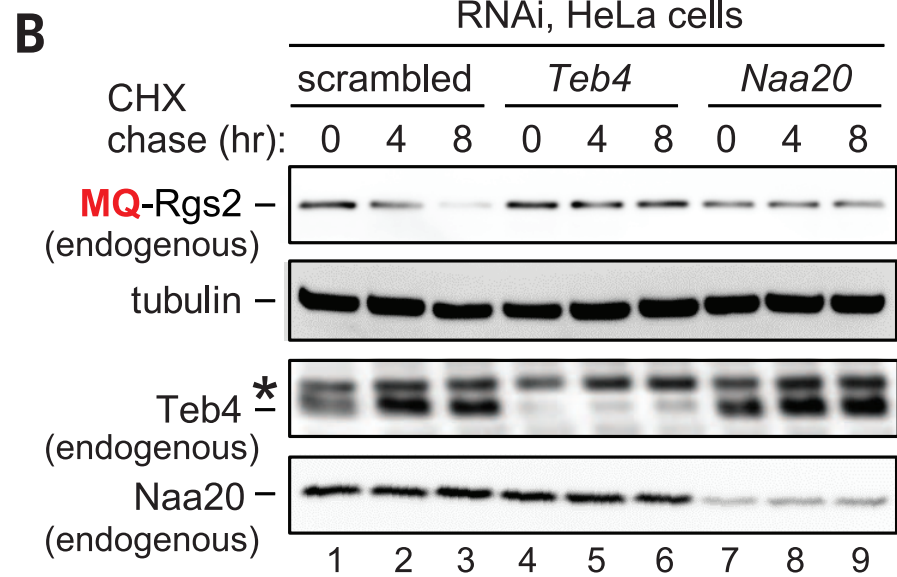
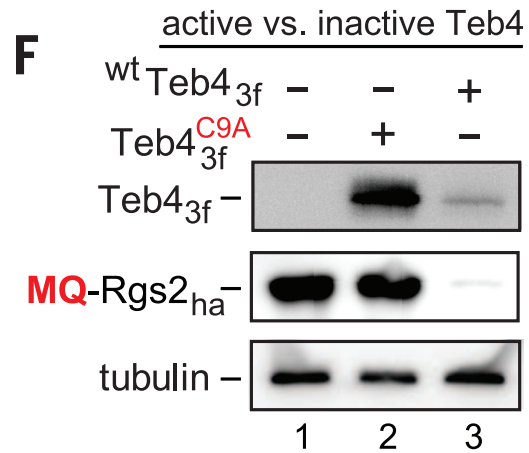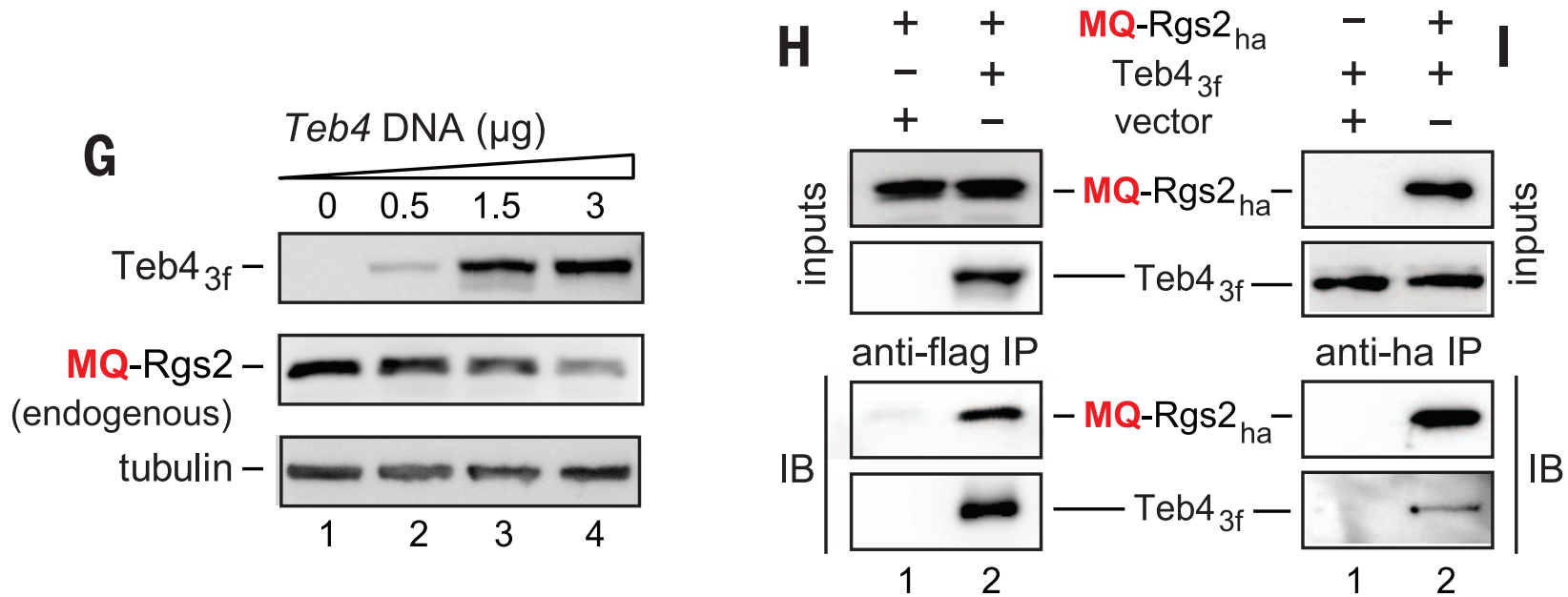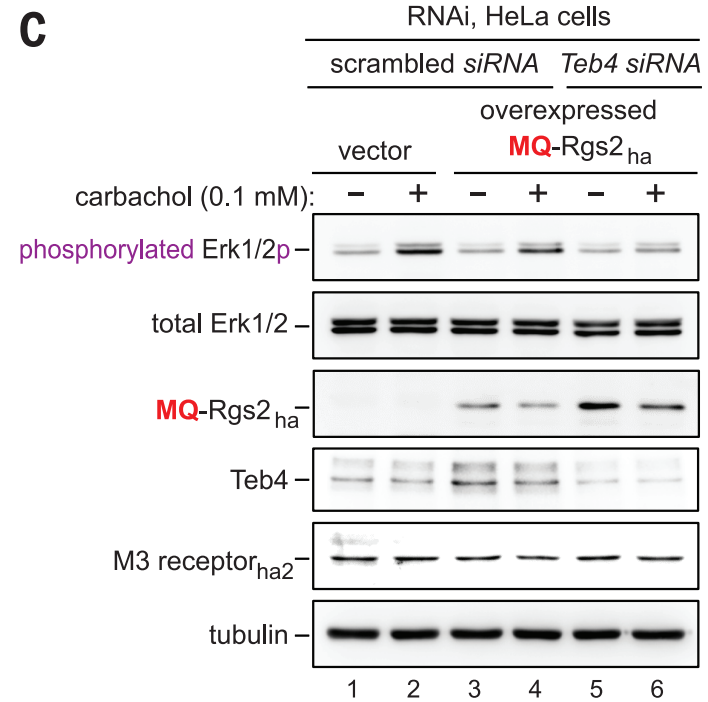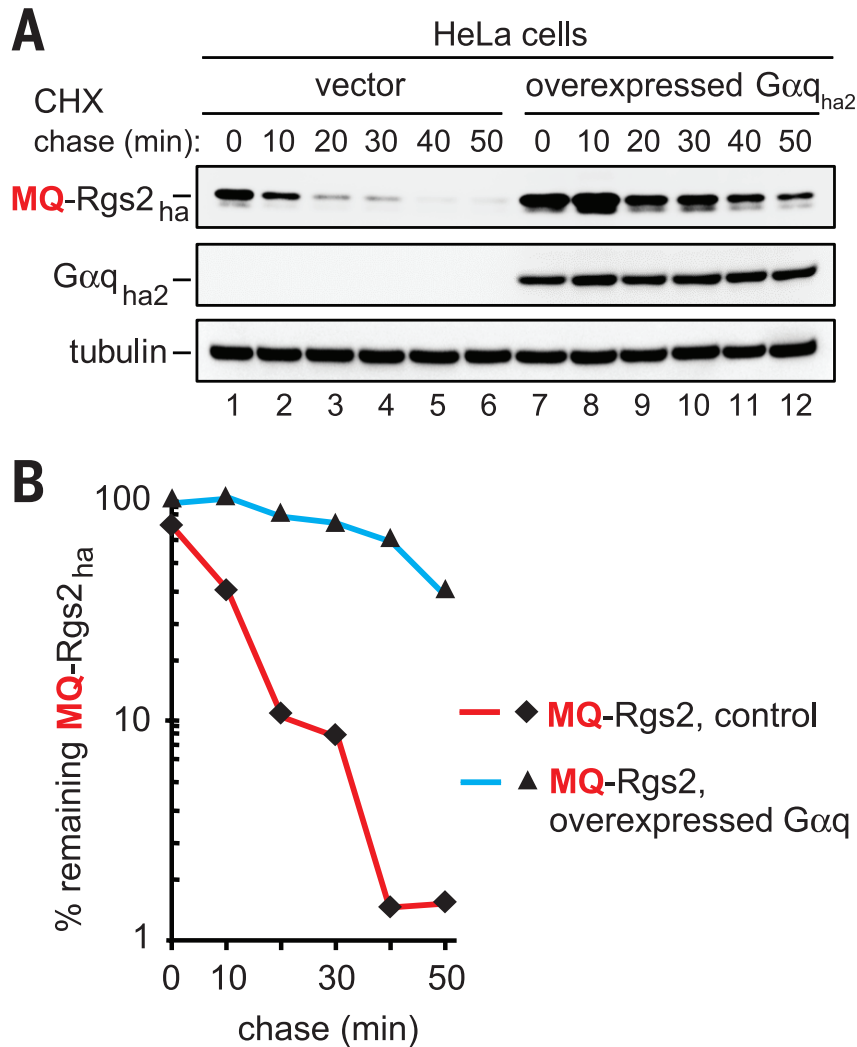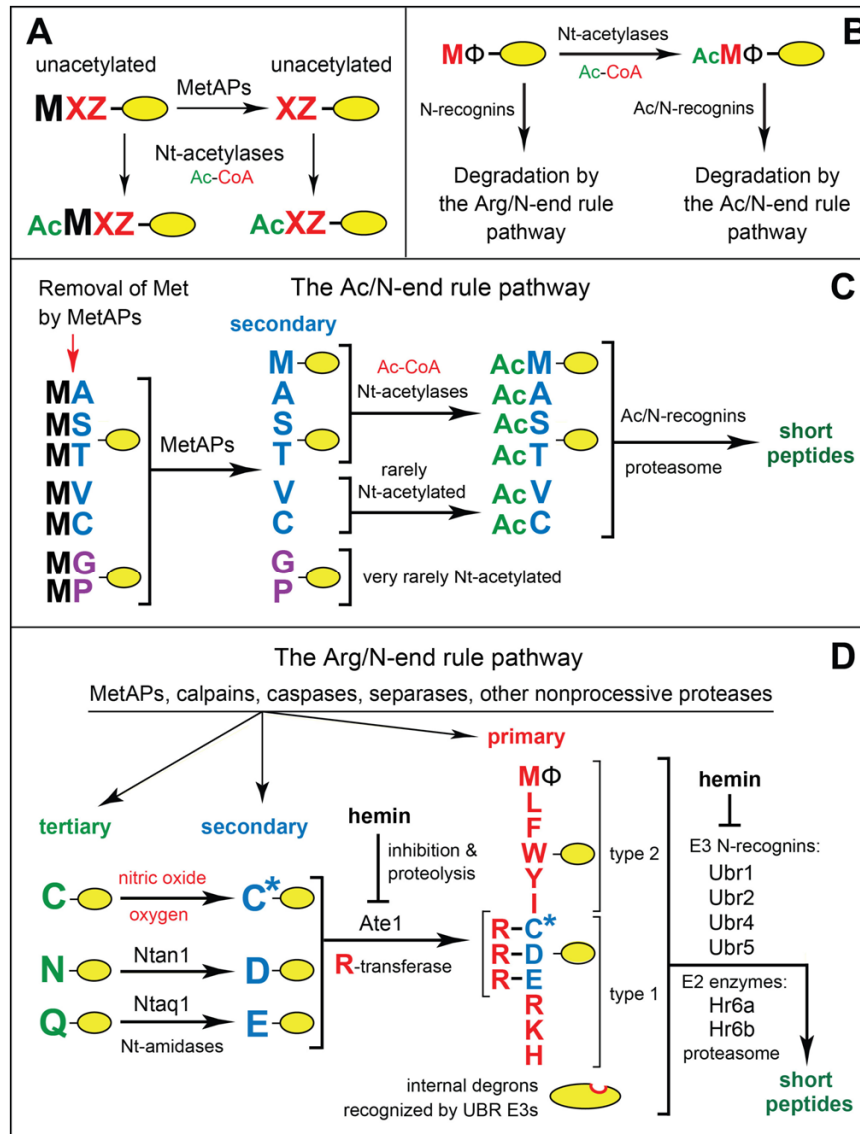**Fig. 3. Gα$_q$ stabilizes Rgs2 while the Teb4-mediated degradation of Rgs2 increases signaling by Gα$_q$.** (**A**) CHX chase of MQ-Rgs2$_{ha}$ in HeLa cells that did not express or overexpressed the HA-tagged Gα$_q$. (**B**) Quantification of data in (A). See the legend to fig. S3 for definitions of "100%" levels at zero time. (**C**) HeLa cells were subjected to RNAi either for a "scrambled" target or for Teb4. The M3 receptor was transiently expressed either alone or together with MQ-Rgs2$_{ha}$. The levels of indicated proteins, including the levels of either total Erk1/2 or the activated (specifically phosphorylated) Erk1/2p, were determined by SDS-PAGE and immunoblotting of cell extracts that had been prepared 10 min after treatment of cells with carbachol.

Fig. S1. Conditional removal of N-terminal methionine from nascent proteins, their N-terminal acetylation, and the N-end rule pathway.

(**A**) N-terminal processing of nascent proteins by N^α-terminal acetylases (Nt-acetylases) and Met-aminopeptidases (MetAPs). "**Ac**" denotes the N^α-terminal acetyl moiety. **M**, methionine (Met) residue. **X** and **Z**, single-letter abbreviations for any amino acid residue. Yellow ovals denote the rest of a protein molecule. MetAPs cotranslationally remove N-terminal Met from a nascent protein unless the side chain of a residue at position 2 is bulkier than Val, in which case Met is retained (*12, 34*).

(**B**) Functional complementarity between the Arg/N-end rule pathway and the Ac/N-end rule pathway for proteins bearing the N-terminal **MΦ** motif, i.e., unacetylated N-terminal Met followed by a bulky hydrophobic (Φ) residue. This motif is targeted by the Arg/N-end rule pathway (*16*). Because the Met-Φ motif is also a substrate of the NatC Nt-acetylase (Fig. S2), Met-Φ proteins are usually Nt-acetylated at least in part, thereby acquiring the previously characterized Ac/N-degrons (*13, 16*). Thus, *both* Nt-acetylated and unacetylated versions of the same Met-Φ protein can be destroyed, either by the Ac/N-end rule pathway or by the "complementary" Arg/N-end rule pathway (*16*).

(**C, D**) The mammalian N-end rule pathway. The main determinant of an N-degron is a destabilizing N-terminal residue of a protein. Recognition components of the N-end rule pathway, called N-recognins, are E3 ubiquitin ligases that can recognize N-degrons.
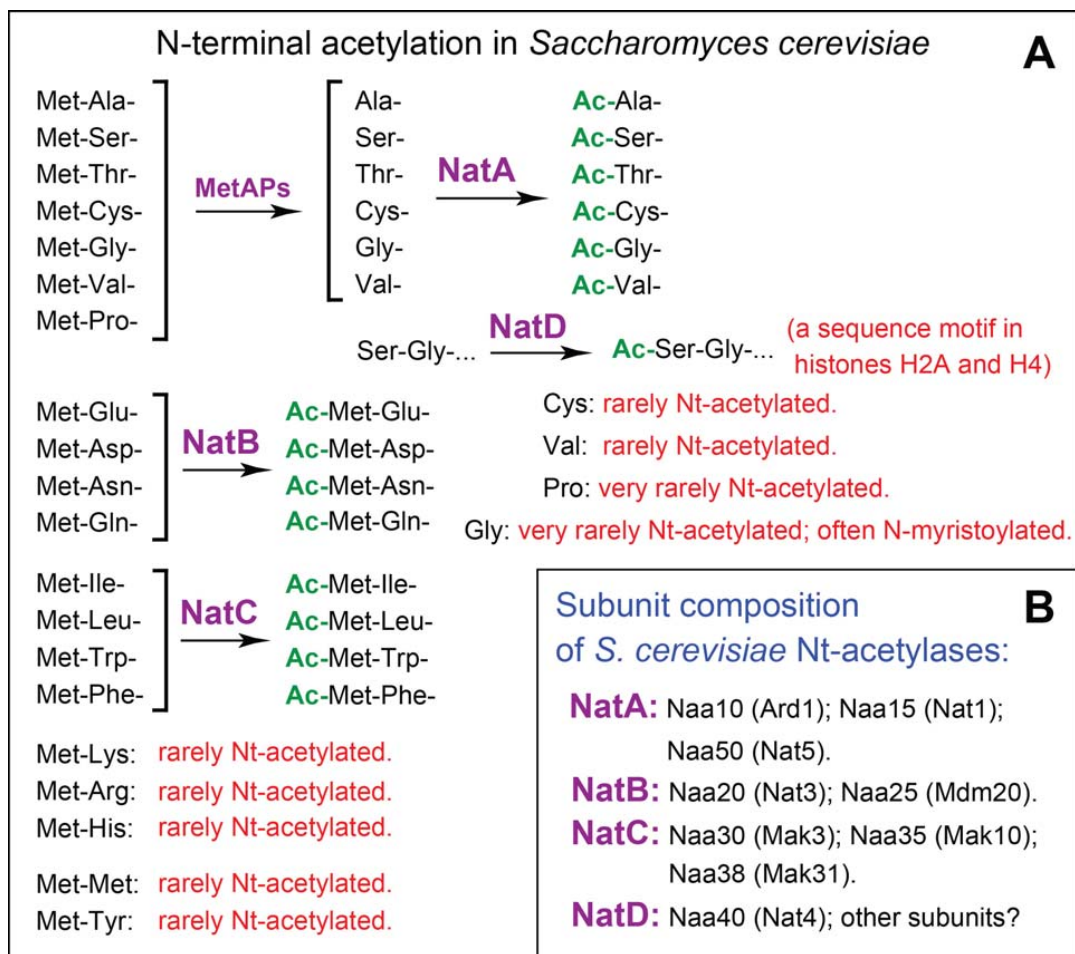
Regulated degradation of proteins or their fragments by the N-end rule pathway mediates a strikingly broad range of functions, including the sensing of heme, nitric oxide, oxygen, and short peptides; control of protein quality and subunit stoichiometries, including the elimination of misfolded proteins; regulation of signaling by G proteins; repression of neurodegeneration; regulation of apoptosis, chromosome cohesion/segregation, transcription, and DNA repair; control of peptide import; regulation of meiosis, autophagy, immunity, fat metabolism, cell migration, actin filaments, cardiovascular development, spermatogenesis, and neurogenesis; the functioning of adult organs, including the brain, muscle and pancreas; and the regulation of many processes in plants (references (*12-14, 16, 18, 20, 35-88*) and references therein). In eukaryotes, the N-end rule pathway consists of two branches, the Ac/N-end rule pathway and the Arg/N-end rule pathway.

(**C**) The Ac/N-end rule pathway. This diagram illustrates the mammalian Ac/N-end rule pathway through extrapolation from its *S. cerevisiae* version. As described in the main text, the Ac/N-end rule pathway has been identified only in *S. cerevisiae* (*13, 15, 16*), i.e., the presence of this pathway in mammals and other multicellular eukaryotes was conjectural, until the present work. Red arrow on the left indicates the removal of N-terminal Met by Met-aminopeptidases (MetAPs). N-terminal Met is retained if a residue at position 2 is nonpermissive (too large) for MetAPs. If the retained N-terminal Met or N-terminal Ala, Ser, Thr are followed by acetylation-permissive residues, the above N-terminal residues are N^{α}-terminally acetylated (Nt-acetylated) by ribosome-associated Nt-acetylases (*21, 89, 90*). Nt-terminal Val and Cys are Nt-acetylated relatively rarely, while N-terminal Pro and Gly are almost never Nt-acetylated. (N-terminal Gly is often N-myristoylated.) N-degrons and N-recognins of the Ac/N-end rule pathway are called Ac/N-degrons and Ac/N-recognins, respectively (*12*). The term "secondary" refers to Nt-acetylation of a destabilizing N-terminal residue before a protein can be recognized by a cognate Ac/N-recognin. As described in the main text, the human Teb4 E3 ubiquitin ligase was identified, in the present study, as an Ac/N-recognin of the mammalian Ac/N-end rule pathway. Natural Ac/N-degrons are regulated at least in part by their reversible steric shielding in protein complexes (*15, 16*).

(**D**) The Arg/N-end rule pathway. The prefix "Arg" in the pathway's name refers to N-terminal arginylation (Nt-arginylation) of N-end rule substrates by the Ate1 arginyltransferase (R-transferase), a significant feature of this proteolytic system. The Arg/N-end rule pathway targets specific unacetylated N-terminal residues. In the yeast *S. cerevisiae*, the Arg/N-end rule pathway is mediated by the Ubr1 N-recognin, a 225 kDa RING-type E3 ubiquitin ligase and a part of the targeting apparatus comprising a complex of the Ubr1-Rad6 and Ufd4-Ubc4/5 holoenzymes (*12, 14, 18*). In multicellular eukaryotes several functionally overlapping E3 ubiquitin ligases (Ubr1, Ubr2, Ubr4, Ubr5) function as N-recognins of this pathway. An N-recognin binds to the "primary" destabilizing N-terminal residues Arg, Lys, His, Leu, Phe,

Tyr, Trp and Ile. In contrast, the N-terminal Asn, Gln, Asp, and Glu residues (as well as Cys, under some metabolic conditions) are destabilizing owing to their preliminary enzymatic modifications. These modifications include the Nt-deamidation of N-terminal Asn and Gln by the Ntan1 and Ntaq1 Nt-amidases, respectively, and the Nt-arginylation of N-terminal Asp and Glu by the Ate1 R-transferase, which can also Nt-arginylate oxidized Cys, either Cys-sulfinate or Cys-sulfonate. They can form in animal and plant cells through oxidation of Cys by nitric oxide (NO) and oxygen, and also by N-terminal Cys-oxidases (*19, 44, 52, 59, 61, 91-93*). In addition to its type-1 and type-2 binding sites that recognize, respectively, the basic and bulky hydrophobic unacetylated N-terminal residues, an N-recognin such as Ubr1 contains other substrate-binding sites as well. These sites recognize substrates that are targeted through their internal (non-N-terminal) degrons, as indicated on the diagram (*12*). Hemin (Fe^{3+}-heme) binds to the Ate1 R-transferase, inhibits its Nt-arginylation activity and accelerates its in vivo degradation. Hemin also binds to Ubr1 (and apparently to other N-recognins as well) and alters its functional properties, in ways that remain to be understood (*43*). As shown in the diagram, the unacetylated Met of the N-terminal **MΦ** motif is recognized by both yeast and mammalian Ubr1; this capability greatly expands the substrate range of the Arg/N-end rule pathway (*16*).
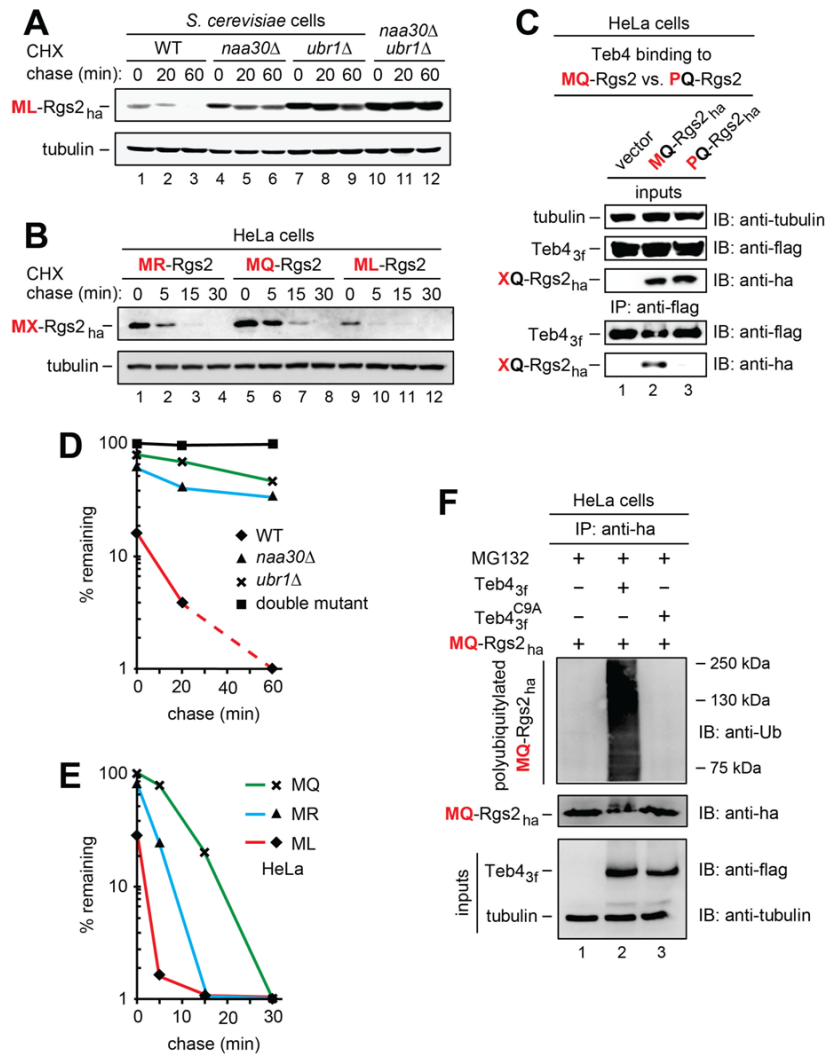
Fig. S2. Specificities and subunit compositions of N$^\alpha$-terminal acetylases (Nt-acetylases).

(**A**) Substrate specificities of *S. cerevisiae* Nt-acetylases. "**Ac**" denotes the N$^\alpha$-terminal acetyl moiety. The bulk of Nt-acetylases are associated with ribosomes (*94, 95*). The specificities of mammalian Nt-acetylases are similar to those of their yeast counterparts, but an individual mammalian genome encodes more than ten Nt-acetylases, in contrast to four in *S. cerevisiae*. Some mammalian Nt-acetylases, such as NatF (its catalytic subunit is called Naa60 (see fig. S4H, I)) (*22*), can Nt-acetylate N-terminal motifs that include Met-Lys or Met-Arg, which are rarely if ever Nt-acetylated in *S. cerevisiae*. This compilation of Nt-acetylases and their specificities is derived from data in the literature ((*21, 89, 90, 96-108*) and references therein).

(**B**) Subunits of *S. cerevisiae* Nt-acetylases. This paper employs the revised nomenclature for subunits of Nt-acetylases (*109*) and cites older names of these subunits in parentheses.

Fig. S3. The targeting of MX-Rgs2 proteins by the yeast and human Ac/N-end rule and Arg/N-end rule pathways.

(**A**) CHX chases with the hypertension-associated mutant human **ML**-Rgs2$_{ha}$ in wild-type, *naa30Δ*, *ubr1Δ*, and *naa30Δ ubr1Δ S. cerevisiae*.

(**B**) As in **A** but in human HeLa cells with wild-type human **MQ**-Rgs2$_{ha}$ and hypertension-associated mutants **MR**-Rgs2$_{ha}$ and **ML**-Rgs2$_{ha}$.

(**C**) HeLa cells expressing **MQ**-Rgs2$_{ha}$ or **PQ**-Rgs2$_{ha}$ together with Teb4$_{3f}$ were treated with a cell-penetrating crosslinker, followed by immunoprecipitations with anti-flag, reversal of crosslinks, SDS-PAGE, and immunoblotting with anti-ha and anti-flag (see also Fig. 2H and Materials and Methods). Note the coimmunoprecipitation of **MQ**-Rgs2$_{ha}$ with Teb4$_{3f}$, and the absence of coimmunoprecipitation of **PQ**-Rgs2$_{ha}$.
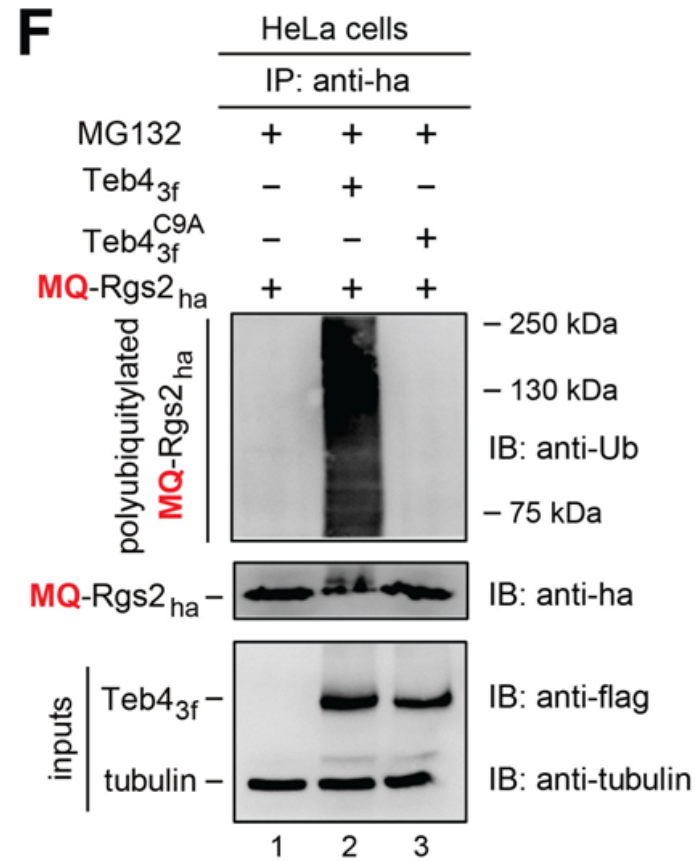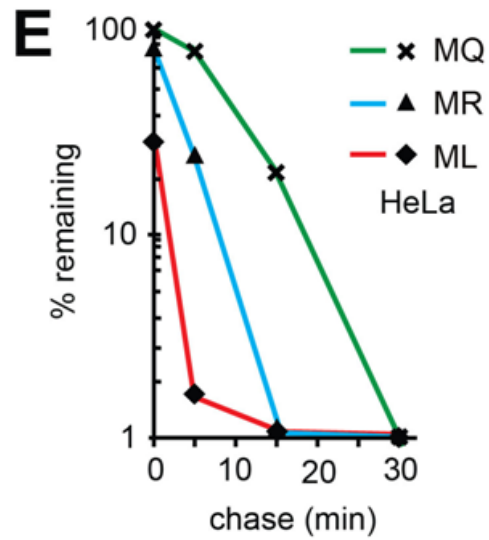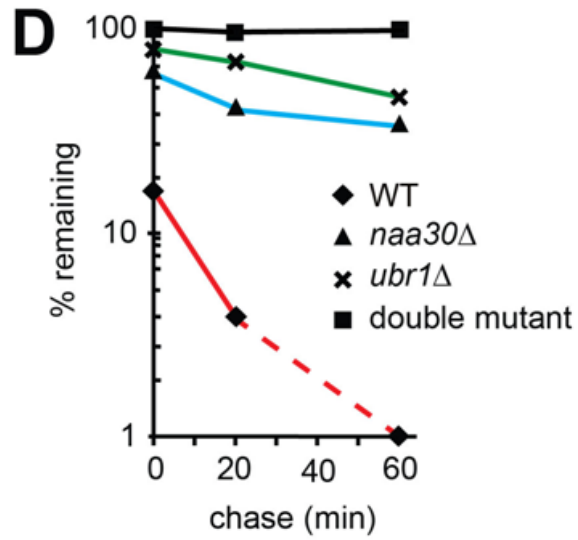
(**D**) Quantification of data in **A**. 100% corresponded to the zero-time level of **ML**-Rgs2$_{ha}$ in *naa30Δ ubr1Δ S. cerevisiae.*

(**E**) Quantification of data in **B**. 100% corresponded to the zero time level of **PQ**-Rgs2$_{ha}$ in HeLa cells.

In every set of degradation curves shown in this figure and in the main Figs. 1 and 3, 100% at zero time was chosen to correspond to the relative initial level of the most slowly degraded test protein in a given set. Panel **A** (quantified in **D**) and panel **B** (quantified in **E**) show the results of CHX-chases that were independently carried out counterparts of CHX-chases that are shown in the main Fig. 1**B** (quantified in **D**) and 1**F** (quantified in **E**), respectively. These comparisons illustrate qualitative reproducibility of independently generated data (particularly the robustly reproduced order of metabolic stabilities of specific test proteins in specific genetic backgrounds), which differed in relatively minor aspects of corresponding degradation curves. In our extensive experience with repeated CHX-chases and ^{35}S-pulse-chases in either *S. cerevisiae* or HeLa cells, a strictly quantitative reproducibility of independently produced and measured chase-degradation patterns remains the aim to be reached.

(**F**) Extracts from HeLa cells expressing **MQ**-Rgs2$_{ha}$ in the presence or absence of coexpressed Teb4$_{3f}$ or Teb4$_{3f}^{C9A}$ and in the presence of the MG132 proteasome inhibitor, as indicated. **MQ**-Rgs2$_{ha}$ was immunoprecipitated from extracts using anti-ha antibody, followed by SDS-PAGE and immunoblotting with anti-ubiquitin antibody to detect polyubiquitin chains linked to **MQ**-Rgs2, and with anti-flag, anti-ha and anti-tubulin antibodies as well, as shown.

A

S. cerevisiae cells

CHX   WT   naa30Δ   ubr1Δ   naa30Δ ubr1Δ
chase (min):   0   20 60   0   20 60   0   20 60   0   20 60

ML-Rgs2ha–

tubulin –

                1   2   3   4   5   6   7   8   9 10 11 12

B

HeLa cells

CHX   **MR**-Rgs2   **MQ**-Rgs2   **ML**-Rgs2
chase (min):   0   5 15 30   0   5 15 30   0   5 15 30

MX-Rgs2ha–

tubulin –

                1   2   3   4   5   6   7   8   9 10 11 12

C

HeLa cells

Teb4 binding to
MQ-Rgs2 vs. **PQ**-Rgs2

vector   **MQ**-Rgs2ha   **PQ**-Rgs2ha

inputs

tubulin –   IB: anti-tubulin

Teb4₃f –   IB: anti-flag

XQ-Rgs2ha–   IB: anti-ha

IP: anti-flag

Teb4₃f –   IB: anti-flag

XQ-Rgs2ha–   IB: anti-ha

                1   2   3

D

WT ◆
naa30Δ ▲
ubr1Δ ✕
double mutant ■

E

MQ ✕ (green)
MR ▲ (blue)
ML ◆ (red)

HeLa

F

HeLa cells
IP: anti-ha

MG132	+	+	+
Teb4$_{3f}$	–	+	–
Teb4$_{3f}^{C9A}$	–	–	+
MQ-Rgs2$_{ha}$	+	+	+

polyubiquitylated **MQ**-Rgs2$_{ha}$

– 250 kDa

– 130 kDa

IB: anti-Ub

– 75 kDa

MQ-Rgs2$_{ha}$ –   IB: anti-ha

inputs

Teb4$_{3f}$ –   IB: anti-flag

tubulin –   IB: anti-tubulin

1   2   3

Fig. S4. Degradation assays with MX-Rgs2 proteins in HeLa cells subjected to RNAi of specific Nt-acetylases and Teb4.

(**A**) CHX-chases with endogenous (not overexpressed) **MQ**-Rgs2 in HeLa cells subjected to RNAi-mediated knockdowns of endogenous Teb4 or Naa20 (NatB).

(**B**) Same as in **A** but CHX-chases with transiently expressed (exogenous) **MQ**-Rgs2$_{ha}$.

(**C**) Relative steady-state levels of exogenous wild-type **MQ**-Rgs2$_{ha}$ and its **MR**-Rgs2$_{ha}$ and **ML**-Rgs2$_{ha}$ mutants in HeLa cells transfected with equal amounts of **MX**-Rgs2$_{ha}$ plasmids.

(**D**) **ML**-Rgs2$_{ha}$ expressed in HeLa cells in the presence of the coexpressed wild-type Teb4$_{3f}$ or Teb4$_{3f}^{C9A}$. Note a strong decrease of **ML**-Rgs2$_{ha}$ in the presence of wild-type Teb4$_{3f}$ but not in the presence of its inactive missense mutant Teb4$_{3f}^{C9A}$. Note also a much lower steady-state level of active Teb4$_{3f}$ (in comparison to the inactive Teb4$_{3f}^{C9A}$), owing to the previously described self-targeting of active Teb4 for degradation (*24*).
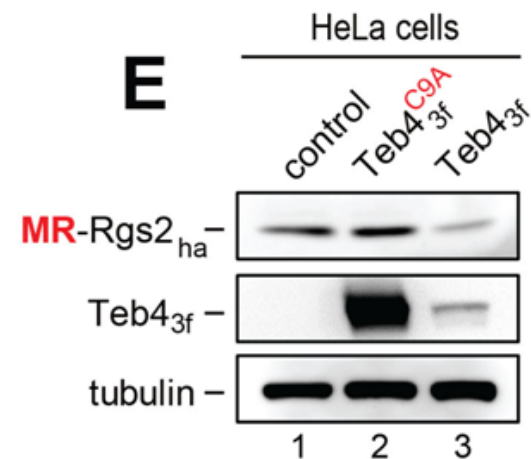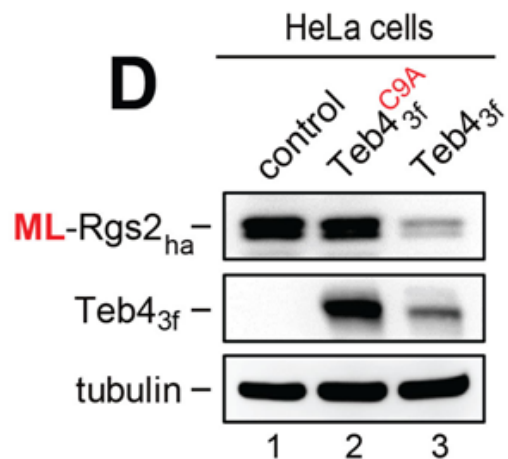
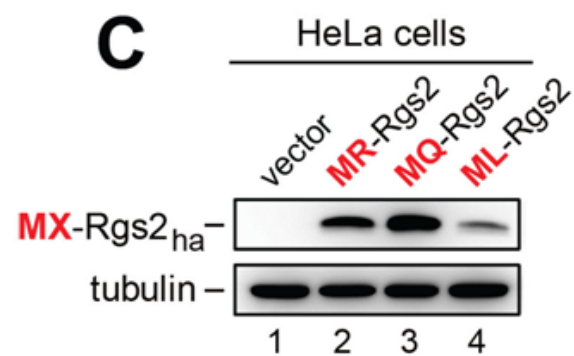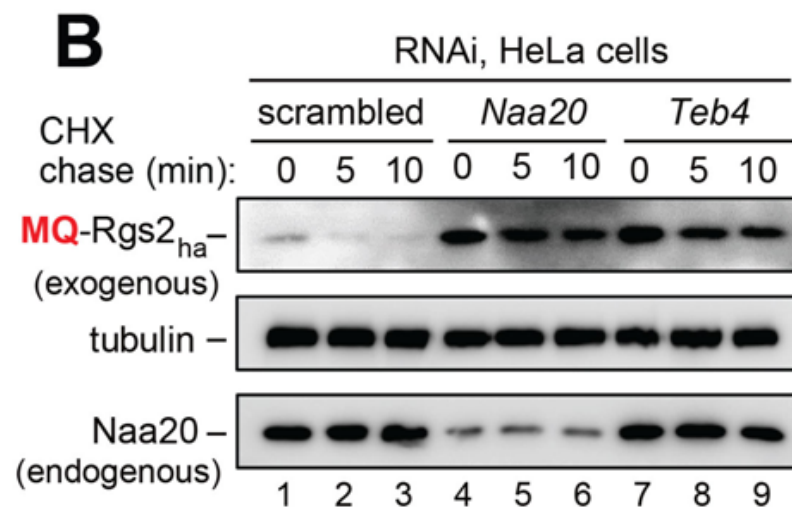(**E**) Same as in **D** but with **MR**-Rgs2$_{ha}$.

(**F**) Quantification of data in **C** (relative levels of the three **MX**-Rgs2$_{ha}$ proteins).

(**G**) Same as in **F** but quantification, using qRT-PCR, of the relative levels of mRNAs encoding the three **MX**-Rgs2$_{ha}$ proteins. Standard errors of means (SEMs), with qRT-PCR assays in triplicate for each sample, are indicated as well.

(**H**) Steady-state levels of transiently expressed (exogenous) **MR**-Rgs2$_{ha}$ in HeLa cells subjected to RNAi-mediated knockdowns of either endogenous Naa60, the cognate (for **MR**-Rgs2$_{ha}$) NatF Nt-acetylase, or endogenous Naa20, the non-cognate (for **MR**-Rgs2$_{ha}$) NatB Nt-acetylase. Note the increase in **MR**-Rgs2$_{ha}$ in response to RNAi of Naa60 but not of Naa20.

(**I**) Same as in **H** but with **MK**-Rgs2$_{ha}$, a derivative of wild-type **MQ**-Rgs2$_{ha}$ not encountered, thus far, among human patients, that contained another basic residue at position 2.

(**J**) ^{35}S-pulse-chases with **MX**-Rgs2$_{ha}$ (**X**=R, Q, L) in HeLa cells.

A RNAi, HeLa cells

CHX chase (hr):
scrambled: 0 4 8
Teb4: 0 4 8
Naa20: 0 4 8

MQ-Rgs2 (endogenous)

Teb4 (endogenous)

Naa20 (endogenous)

tubulin

1 2 3 4 5 6 7 8 9

B RNAi, HeLa cells

CHX chase (min):
scrambled: 0 5 10
Naa20: 0 5 10
Teb4: 0 5 10

MQ-Rgs2ha (exogenous)

tubulin

Naa20 (endogenous)

1 2 3 4 5 6 7 8 9

C HeLa cells

vector, **MR**-Rgs2, **MQ**-Rgs2, **ML**-Rgs2

MX-Rgs2ha

tubulin

1 2 3 4

D HeLa cells

control, Teb4$_{3f}^{C9A}$, Teb4$_{3f}$

ML-Rgs2ha

Teb4$_{3f}$

tubulin

1 2 3

E HeLa cells

control, Teb4$_{3f}^{C9A}$, Teb4$_{3f}$

MR-Rgs2ha

Teb4$_{3f}$

tubulin

1 2 3

F

MX-Rgs2 protein level (%)

G

MX-Rgs2 mRNA level (%)

H

RNAi, HeLa cells

scrambled / Naa20 / Naa60

MR-Rgs2ha –
Naa60 –
Naa20 –
tubulin –

1   2   3

I

RNAi, HeLa cells

scrambled / Naa20 / Naa60

MK-Rgs2ha –
Naa60 –
Naa20 –
tubulin –

1   2   3

J

HeLa cells

MR-Rgs2   MQ-Rgs2   ML-Rgs2

^{35}S-chase (hr):   0 0.5 1 2   0 0.5 1 2   0 0.5 1 2

MX-Rgs2ha –

1 2 3 4   5 6 7 8   9 10 11 12

Fig. S5. Mass spectrometric analyses of Nt-acetylation of MQ-Rgs2 and MQ-Rgs2$^{1-10}$-[GST]. (**A**) Wild-type **MQ**-Rgs2$_{ha}$ purified from human HEK293 cells is Nt-acetylated. (**B**) Non-Nt-acetylated (upper panel) and Nt-acetylated **MQ**-Rgs2$^{1-10}$-[GST] fusion (lower panel) purified from *E. coli* that either lacked or expressed, respectively, the *Schizosaccharomyces pombe* NatB Nt-acetylase (see Materials and Methods).

Fig. S6. Rgs2, Teb4, N-terminal acetylation, and the N-end rule pathway. Rgs2 and Teb4 are, respectively, a substrate and Ac/N-recognin of the mammalian Ac/N-end pathway. Only some Rgs2-regulated processes (including the $G\alpha_q$-mediated activation of Erk1/2 kinase) are shown. Both wild-type **MQ**-Rgs2 and its hypertension-associated mutant **MR**-Rgs2 (the latter is not shown) are Nt-acetylated and conditionally destroyed by the Teb4-mediated Ac/N-end rule pathway. In contrast, another hypertension-associated mutant, **ML**-Rgs2, is targeted by both the Ac/N-end rule pathway and the Arg/N-end rule pathway (see the main text) (fig. S1C, D). Some abbreviations: IP_3, inositol trisphosphate. DAG, diacyglycerol.

RGS proteins as either identified or possible N-end rule substrates.

Identified RGS N-end rule substrates:

RGS proteins	N-termini	Degradation by the Arg/N-end rule pathway	Degradation by the Ac/N-end rule pathway
MQ-Rgs2, wild-type **1**	**MQ**SAMF-1	No	Yes (Ac**MQ**SAMF-)
MR-Rgs2, mutant (hypertension-associated) **2**	**MR**SAMF-1	No	Yes (Ac**MR**SAMF-)
ML-Rgs2, mutant (hypertension-associated) **3**	**ML**SAMF-1	Yes (**ML**SAMF-) unacetylated	Yes (Ac**ML**SAMF-)
CK-Rgs4, wild-type **4**	M^γ**CK**GLA-1	Yes (Arg**C*K**GLAG-) Cys: oxidized, arginylated	Possibly, to a minor extent, if Cys is also Nt-acetylated
CK-Rgs5, wild-type **5**	M^γ**CK**GLA-1	Yes (Arg**C*K**GLAA-) Cys: oxidized, arginylated	Possibly, to a minor extent, if Cys is also Nt-acetylated
CK-Rgs16, wild-type **6**	M^γ**CR**TLA-1	Yes (Arg**C*R**TLAA-) Cys: oxidized, arginylated	Possibly, to a minor extent, if Cys is also Nt-acetylated

Possible (predicted) RGS N-end rule substrates:

RGS proteins	N-termini	Degradation by the Arg/N-end rule pathway	Degradation by the Ac/N-end rule pathway
MR-Rgs1, wild-type **7**	**MR**AAAI-1	No	Yes (Ac**MR**AAAI-)
AQ-Rgs6, wild-type **8**	M^γ**AQ**GSG-1	No	Yes (Ac**AQ**GSG-)
AQ-Rgs7, wild-type **9**	M^γ**AQ**GNN-1	No	Yes (Ac**AQ**GNN-)
AA-Rgs8, wild-type **10**	M^γ**AA**LLM-1	Unclear	Yes (Ac**AA**LLM-)
MF-Rgs12, wild-type **11**	**MF**RAGE-1	Yes (**MF**RAGE-) unacetylated	Yes (Ac**MF**RAGE-)
SR-Rgs13, wild-type **12**	M^γ**SR**RNC-1	No	Yes (Ac**SR**RNC-)
MR-Rgs17, wild-type **13**	**MR**KRQQ-1	No	Yes (Ac**MR**KRQQ-)

Fig. S7. Mammalian RGS proteins as identified or predicted N-end rule substrates.
Human RGS proteins as identified or possible (predicted) substrates of either the Ac/N-end rule pathway, or the Arg/N-end rule pathway, or both pathways at the same time, depending on the Nt-acetylation status of a specific RGS protein. See also the main text.

Table S1. *S. cerevisiae* strains used in this study.

Strains	Relevant genotypes	Sources
JD53	*MATα trp1- 63 ura3-52 his3- 200 leu2-3112. lys2-801*	(*110*)
BY4742	*MATα his3-1 leu2-0 lys2-0 ura3-0 can1-100*	Open Biosystems, Inc.
CHY223	*doa10Δ::kanMX6* in JD53	(*13*)
CHY272	*naa30Δ::kanMX4* in BY4742	Open Biosystems, Inc.
CHY345	*ubr1Δ::LEU2* in BY4742	(*16*)
CHY349	*naa30Δ::kanMX4 ubr1Δ::LEU2* in BY4742	(*16*)
CHY367	*naa20Δ::natNT2* in JD53	This study

Table S2. Plasmids used in this study.

Plasmids	Descriptions	Sources
pCH12	pET30a	Novagen, Inc.
pCH15	pACYCDuet	Novagen, Inc.
pCH61	pcDNA3.1(+) with ha_2	Hwang's lab collection
pCH692	p316CUP1	Hwang's lab collection
pCH759	Teb4 in pcDNA3.1 myc/His (-)	(*24*)
pCH760	$Teb4^{C9A}$ in pcDNA3.1 myc/His(-)	(*24*)
pCH766	$MQ\text{-}Rgs2_{ha}$ in pcDNA3(+)	(*11*)
pCH767	$ML\text{-}Rgs2_{ha}$ in pcDNA3(+)	(*11*)
pCH768	$MR\text{-}Rgs2_{ha}$ in pcDNA3(+)	(*11*)
pCH821	$MPQ\text{-}Rgs2_{ha}$ in pcDNA3(+)	This study
pCH879	$Teb4_{f3h}$ in pcDNA3.1	This study
pCH881	$Teb4^{C9A}_{f3h}$ in pcDNA3.1	This study
pCH3002	MQ-Rgs2-GST in pACYCDuet	This study
pCH3015	pET30a	Qiagen, Inc.
pCH3025	*S. pombe Naa20$^+$-NAA25$^+$* in pACYCDuet	(*32*)
pCH3056	MQ-Rgs2-GST in pET30a	This study
pCH3080	$MQ\text{-}Rgs2^{1\text{-}10}\text{-}GST$ in pET30a	This study
pCH3132	$M3_{ha2}$ in pcDNA3.1(+)	This study
pCH5050	$MQ\text{-}Rgs2_{ha}$ in pRS316, with P_{CUP1}	This study
pCH5051	$ML\text{-}Rgs2_{ha}$ in pRS316, with P_{CUP1}	This study
pCH5064	$G\alpha q_{ha2}$ in pcDNA3.1(+)	This study

Table S3. Some PCR primers used in this study.

Name	Primer sequences
OCH1091	5'-CTTGGTACCATG CCA CAAAGTGCTATGTTCTTGGCTGTT-3'
OCH1100	5'-AACCTCGAGCTAAGCGTAATCTGGAACATCGTATGGGTAAGAACCTGTAGCATGAGGCTCTGTGGTGAT-3'
OCH1265	5'-GGTAAGCTTGACTATAAAGACCATGACGGTGATTATAAAGATCATGATATCGATTACAAG-3'
OCH1266	5'-AATCTTAAGTTAATGATGGTGATGGTGATGAGAACCCTTGTCATCGTCATCCTTGTAATC-3'
OCH1514	5'-TATCTCGAGTCATTTTGGAGGATGGTCGCCACCACC -3'
OCH3006	5'-TCCCATATGCAAAGTGCTATGTTCTTGGCTGTT-3'
OCH3013	5'-CGCGGATCCTGTAGCATGAGGCTCTGTGGTGAT-3'
OCH3015	5'-CGCGGATCCATGTCCCCTATACTAGGTTATTGG-3'
OCH3095	5'-TCCCATATGCAAAGTGCTATGTTCTTGGCTGTTCAATCCCCTATACTAGGTTATTGG-3'
OCH3178	5'-ACAGGATCCATGACCTTGCACAATAACAGTAC-3'
OCH3179	5'-ACATCTAGACAAGGCCTGCTCGGGTGCGCGCTTG-3'
OCH5070	5'-CCCGGATCCATGCAAAGTGCTATGTTCTTGGCT-3'
OCH5071	5'-CCCGGATCCATGTTAAGTGCTATGTTCTTGGCTGTTCAA-3'
OCH5073	5'-CCCGAGCTCCTAAGCGTAATCTGGAACATCGTATGGGTAGCTAGCTGTAGCATGAGG CTCTGTGGTGAT-3'
OCH5090	5'-GTCGGTACCATGACTCTGGAGTCCATCATGGCG-3'
OCH5091	5'-GCTCTCGAGGACCAGATTGTACTCCTTCAGGTT-3'

Materials and Methods

Reagents and antibodies

Cycloheximide, dithiobis(succinimidylpropionate) (DSP; Lomant's reagent), MG132 and complete protease inhibitor cocktail tablet were from Sigma, Thermo Scientific, Calbiochem and Roche, respectively. Antibodies to the following antigens were used for immunoblotting and/or immunoprecipitation: anti-flag M2 (Sigma, F1804 or Stratagen, 200471), anti-c-Myc-9E10 (Sigma, M5546), anti-hemaggutinin (ha) tag (Sigma, H9658 or H6958), anti-tubulin (Sigma, T5168), anti-Teb4 (Bethyl Laboratories, A304-171A), anti-ubiquitin (Stressgen, SPA-203), anti-Naa20 (Nat5) (Santa Cruz Biotechnology, sc-100645), anti-Naa60 (Nat15) (Abcam, ab103800), anti-phospho-p44/42 Erk1/2 (Cell Signaling Technologies, Ab9101), anti-p44/42 Erk1/2 (Cell Signaling Technologies, Ab9102) and anti-Rgs2 (Abgent, AT3628a). Secondary antibodies for immunoblotting were HRP-conjugated goat anti-rabbit (Bio-Rad, 170-6515) or anti-mouse (Bio-Rad, 170-6516), and either ECL Prime Western Blotting Detection System (GE Healthcare) or Clarity Western ECL substrate (Bio-Rad) were used, according to manufacturers' protocols. The following reagents were used for immunoprecipitation and GST-pulldown assays: anti-flag M2 affinity gel (Sigma, A2220), Dynabeads Protein A and G (Life Technologies), and Glutathione Hicap (Qiagen). For determining the state of N^α-terminal acetylation (Nt-acetylation) of Rgs2, human Rgs2 (purified from the HEK293 cell line) was purchased from Origene (TP302781) and analyzed using mass spectrometric (MS) techniques (see below).

Yeast strains, media, and genetic techniques

The *S. cerevisiae* strains used in this study are described in Table S1. Standard techniques (*27, 28*) were employed for strain construction and transformation. *S. cerevisiae* media included YPD medium (1% yeast extract, 2% peptone, 2% glucose; only most relevant components are cited); SD medium (0.17% yeast nitrogen base, 0.5% ammonium sulfate, 2% glucose); and synthetic complete (SC) medium (0.17% yeast nitrogen base, 0.5% ammonium sulfate, 2% glucose), plus a drop-out mixture of compounds required by a given auxotrophic strain. The *S. cerevisiae* strain CHY367 (*naa20Δ::natNT2*) was constructed using PCR-mediated gene targeting (*29*) and the natNT2 module (*30*) in the strain JD53 (see Table S1).

Cell culture, transfection and RNA interference

Human HeLa cell line was grown in Dulbecco's Modified Eagle Medium (DMEM) (Ronza) supplemented with 10% fetal bovine serum (FBS) (HyClone) and penicillin (100 U/ml)/streptomycin (100 μg/ml) (HyClone) in a 5% CO_2 incubator at 37°C. Transfections with DNA plasmids or siRNA oligoribonucleotides were carried out using Lipofectamine-2000 (Life Technologies) according to the manufacturer's instructions. For RNA interference (RNAi), HeLa cells were seeded on day 1 at 2×10^5 cells per well in 6-well cell culture plates (SPL Life Sciences, Korea) containing DMEM and 10% FCS. After incubations for 24 hr, cells were transfected with 100 nM of either human *Teb4* siRNA, or *Naa20* siRNA, or *Naa60* siRNA, or non-targeting (control) siRNA (Santa Cruz Biotechnology, sc-91789, sc-37007, sc-62662, and sc-93037, respectively), using Lipofectamin-2000 according to the manufacturer's instructions.

DNA constructs and primers

E. coli DH5α strain was used for cloning and maintaining plasmids (Table S1). Solg Pfu-X DNA polymerase (SolGent, Korea) was employed for PCR. The plasmids and PCR

primers used in this study are described in Tables S2 and S3, respectively. To express human **MX**-Rgs2 (**X**=Gln, Leu, Arg) in mammalian cells, we used the pCH766, pCH767 and pCH768 plasmids, which expressed, respectively, **MQ**-Rgs2$_{ha}$, **ML**-Rgs2$_{ha}$ and **MR**-Rgs2$_{ha}$ from the P$_{CMV}$ promoter and were a gift from Dr. R. Neubig (Univ. of Michigan Medical School, East Lansing, MI) (*11*). To construct pCH821, which expressed **PQ**-Rgs2$_{ha}$ (**MPQ**-Rgs2$_{ha}$), the **MPQ**-RGS2$_{ha}$-encoding DNA fragment was produced by PCR from the plasmid pCH766 (Table S2) using the primer pair OCH1091/OCH1100. This fragment was digested with *Kpn*I/*Xho*I and ligated into *Kpn*I/*Xho*I-cut pCH766.

To construct the low copy (*CEN*-based) pCH5050 and pCH5051 plasmids, which expressed **MQ**-Rgs2$_{ha}$ and **ML**-Rgs2$_{ha}$ in *S. cerevisiae* from the P$_{CUP1}$ promoter, the relevant *Rgs2* DNA fragments were amplified from pCH766 using the primer pairs OCH5070/OCH5073 and OCH5071/OCH5073, respectively. The resulting PCR products were digested with *Bam*HI/*Sac*I and ligated into *Bam*HI/*Sac*I-cut pCH692, a pRS316-based low copy plasmid containing the P$_{CUP1}$ promoter.

To construct pCH879 and pCH881, which expressed, from the P$_{CMV}$ promoter in mammalian cells, the wild-type human Teb4 and its catalytically-inactive mutant Teb4^{C9A} (both of them were C-terminally tagged with triple flag plus His$_6$), a DNA sequence encoding the above "double" epitope was produced by annealing the complementary primers OCH1265/OCH1266 (Table S3). The resulting DNA, encoding triple flag plus His$_6$, was digested with *Hin*dIII/*Afl*II and ligated into *Hin*dIII/*Afl*II-cut pCH759 and pCH760, which encoded, respectively Teb4 and Teb4^{C9A} in the pcDNA3.1-myc-His(-) A vector (*24*). The plasmid pCH3056, which encoded full-length **MQ**-Rgs2 whose C-terminus was fused to GST, was constructed by producing, at first, a DNA fragment from pCH766 (Table S2), using PCR and the primer pair OCH3006/OCH3013. This fragment was digested with *Nde*I/*Bam*HI. Furthermore, a DNA fragment was produced by PCR from pGEX4T-3 and the primer pair OCH3015/OCH1514, followed by digestion of the resulting fragment with *Bam*HI/*Xho*I. The above two fragments were ligated into *Nde*I/*Xho*I-cut pET30a, yielding the plasmid pCH3056.

To construct the plasmid pCH3080, which expressed, from the IPTG-inducible *T7lac* promoter in *E. coli*, a fusion between the N-terminal 10 residues of **MQ**-Rgs2 and the GST moiety, a DNA fragment was produced by PCR using pCH3056 (Table S2) and the primer pair OCH3095/OCH1514 (Table S3). The resulting fragment was digested with *Nde*I/*Xho*I and ligated into *Nde*I/*Xho*I-cut pET30a (Table S2).

To construct pCH3132 that expressed the human muscarinic acetylcholine receptor M3 from the P$_{CMV}$ promoter, DNA sequence encoding M3 was PCR-amplified from a human HEK293T cDNA library using primer pairs OCH3178/OCH3179. The resulting PCR fragment was digested with *Bam*HI/*Xba*I and ligated into *Bam*HI/*Xba*I-cut pCH61. To clone pCH5064 that expressed the human guanidine-nucleotide binding protein G(q) subunit alpha (Gαq) from the P$_{CMV}$ promoter, DNA sequence encoding Gαq was also PCR-amplified from HEK293T cDNA library using primer pairs OCH5090/OCH5091. The resulting DNA fragment was digested with *Kpn*I/*Xho*I and ligated into *Kpn*I/*Xho*I-cut pCH61, yielding pCH5064. Construction details for other plasmids are available upon request. All final constructs were verified by DNA sequencing.

Cycloheximide-chase assays and immunoblotting

For immunoblotting, HeLa cells were lysed by incubating them on ice for 20 min in the TLB lysis buffer (1% Triton X100, 50 mM NaCl, 2 mM Na-EDTA, 50 mM Tris-HCl, pH 7.4), containing complete protease inhibitor mixture (Roche). After precipitating cell debris by centrifugation at 11,200*g* for 10 min at 4°C, total protein concentrations in the supernatants were determined using Bradford or DC protein assay (Bio-Rad). Identical total amounts of protein in

each sample were heated at 95°C for 10 min or at 37°C for 15 min (the samples for immunoblotting of Teb4 were incubated, instead, at 37°C for 20 min) in 1x SDS-sample buffer, followed by Tris-glycine-SDS-10% PAGE or Tris-glycine-4-20% PAGE. For immunoblotting analyses of Teb4, protein samples were fractionated by Tris-glycine-SDS-6% PAGE or by Tris-glycine-SDS-8% PAGE. Fractionated proteins were electroblotted to Immobilon-P membranes (Millipore) using mini-transblot cell (Bio-Rad), and were analyzed by immunoblotting with indicated antibodies, followed by secondary antibodies described in the first section above. Immunoblots were detected using Clarity Western ECL substrate (Bio-Rad) or ECL Plus Western blotting Detection System (GE Healthcare).

Cycloheximide (CHX)-chase assays with HeLa cells were set up on day 1 at 2×10^5 cells/well in 6- or 12-well cell culture plates (SPL Life Sciences, Korea) containing DMEM and 10% FCS. After 24-hr incubation at 37°C, the cells were treated with CHX at the final concentration of 0.1 mg/ml, harvested by centrifugation at each time point, and lysed in RIPA buffer (0.1% NP40, 0.15 M NaCl, 5 mM Na-EDTA, 1 mM dithiothreitol (DTT), 50 mM HEPES, pH 7.5, plus the *"complete protease inhibitor cocktail"* (Roche)). Equal amounts of total protein were fractionated by Tris-glycine SDS-4-20 % PAGE, followed by immunoblotting with indicated antibodies. In particular, immunoblotting with antibody to α-tubulin was used as a loading control for all immunoblotting experiments.

CHX-chases with *S. cerevisiae* cells were performed as previously described (*13, 15*), with slight modifications. *S. cerevisiae* were grown to A_{600} of 0.8-1.0 at 30°C in selective media appropriate for a plasmid(s) carried by a strain. Cells were harvested by centrifugation at 11,200*g* for 1 min and thereafter resuspended in fresh YPD to a final concentration of A_{600} of 1.0, followed by the treatment with CHX at the final concentration of 0.2 mg/ml. At indicated times, cell samples (corresponding to 1 ml of cell suspension at A_{600} of 1) were harvested by centrifugation for 1 min at 11,200*g*, and were resuspended in 0.8 ml of 0.2 M NaOH and incubated for 20 min on ice, followed by centrifugation for 1 min at 11,200*g*. Pelleted cells were resuspended in 80 μl of HU buffer (8 M urea, 5% SDS, 1 mM Na-EDTA, 0.1 M DTT, 0.005% bromophenol blue, 0.2 M Tris-HCl, pH 6.8) containing 1x protease inhibitor cocktail *"for use with fungal and yeast extracts"* (Sigma), and heated for 10 min at 70°C. After centrifugation for 5 min at 11,200*g*, 10 μl of supernatant was subjected to SDS-10% PAGE, followed by immunoblotting with anti-ha (1:2,000) and anti-tubulin (1:2,000) antibodies. Quantification of immunoblotting data was carried out using GelQuantNET (http://biochemlabsolutions.com/GelQuantNET.html).

Cycloheximide-chase assays with co-expressed Rgs2ha and Gαqha2
To determine whether Gαqha2, a C-terminally doubly ha-tagged Gαq, could stabilize **MQ**-Rgs2ha against degradation in HeLa cells, cultures at ~90% confluence in 6-well (35-mm) plates were transiently cotransfected with 0.5 μg of pCH766 (expressing **MQ**-Rgs2ha) and 2.5 μg of either pCH5064 (expressing Gαqha2) or pCH61 (vector alone) per well, in the serum-free Opti-MEM medium (Gibco). After 5-hr transfection, the medium was replaced by DMEM containing 10% FBS. After incubation for 24 hr at 37°C, the cells were treated with CHX at the final concen tration of 0.1 mg/ml, harvested by centrifugation at each time point of a chase, and lysed in RIPA buffer (0.1% NP40, 0.15 M NaCl, 5 mM Na-EDTA, 1 mM dithiothreitol (DTT), 50 mM HEPES, pH 7.5, plus the *"complete protease inhibitor cocktail"* (Roche)). Equal amounts of total protein were fractionated by Tris-glycine SDS-12 % PAGE, followed by immunoblotting with anti-ha or anti-tubulin antibodies. Immunoblotting with antibody to α-tubulin was used as a loading control for all immunoblotting experiments.

³⁵S-pulse-chase assays

^{35}S-pulse-chase assays

HeLa cell cultures (at ~75% confluence) were transfected with 2.5 μg of a plasmid per 35-mm well, using Lipofectamine-2000 according to the manufacturer's protocol. 48 hr after transfection cells were pulse-labeled for 15 min with [^{35}S]-L-methionine (0.1 mCi/ml, MP Biomedicals) in DMEM lacking methionine. CHX and 5 mM unlabeled methionine were then added to the final concentration of 0.1 mg/ml and 5 mM, respectively. Cells in an entire 35-mm well were lysed at the indicated time points of a chase by rapid scraping into 0.1 ml of TSD buffer (1% SDS, 5mM DTT, 50 mM Tris-HCl, pH7.4) and snap-freezing in liquid nitrogen. Samples were then heated at 95°C for 10 min and diluted with 10 volumes of TNN buffer (0.5% NP40, 0.25M Na Cl, 5 mM Na-EDTA, 50 mM Tris-HCl, pH 7.4) containing the *"complete protease-inhibitor mixture"* (Roche). The amounts of ^{35}S in the 10% CCl$_3$COOH-insoluble fraction of each sample were then measured by liquid scintillation counting. For immunoprecipitation, the samples were adjusted to contain equal amounts of total ^{35}S and then added to 20 μl of anti-ha agarose (Sigma). Suspensions of beads were incubated by rocking at 4°C for 2 hr, washed 3 times in TNN buffer, and once in 10 mM Tris-HCl, pH 8.5. Final samples were eluted by 30 μl of SDS-PAGE sample buffer, including the heating at 95°C for 5 min, followed by clarification through centrifugation at 11,200*g* for 1 min. 10 μl of each of the resulting samples were separated by SDS-4-20% PAGE (Bio-Rad, followed by autoradiography using Typhoon 9400 PhosphorImager (GE Healthcare) and quantification of autoradiograms with ImageQuant (GE Healthcare).

RNA isolation and quantitative RT-qPCR

Total RNA was isolated from HeLa cells using an RNeasy Mini kit (Qiagen), according to the manufacturer's instructions. 2 μg of total RNA was reverse-transcribed into cDNA with oligo-dT as a primer by using Promega cDNA reverse transcription kit. Quantitative real-time PCR was performed in 20-μl reactions containing 10 ng of the cDNA sample, 50 nM forward and reverse primers, and the SYBR Green Master Mix (Applied Biosystems). Primers for human *Rgs2* and β-actin genes were designed using GenScript Real-time PCR Primer Design tool. Reaction mixtures were incubated at 95°C for 10 min, followed by 40 cycles of 95°C for 15 sec and 60°C for 1 min. No template control sample was included, to enable detection of RNA and/or DNA contamination. Quantification of relative *Rgs2* mRNA expression levels was carried out using the threshold-cycle difference method (ref. (*31*) and *Applied Biosystems StepOne and StepOnePlus Real-Time PCR Systems Getting Started Guide for Relative Standard Curve and Comparative CT experiments*), with β-actin as a normalization control. The *Rgs2* and β-actin gene primer pairs for RT-qPCR were OCH5082/OCH5083 and OCH5084/OCH5085, respectively (Table S3).

***In vivo* ubiquitylation assay**

HeLa cells were transfected with pcDNA3.1 (control vector), or CH776 (a pcDNA3.1-based plasmid expressing **MQ**-Rgs2$_{ha}$), or pCH879 (expressing Teb4$_{3f}$) or pCH881 (expressing Teb4$_{3f}^{C9A}$) (Table S2). After 24 hr, transfected cells were treated with 10 μM MG132 for 4 hr and thereafter lysed with RIPA buffer. Supernatants were immunoprecipitated with a monoclonal anti-ha antibody (Sigma), and were washed three times in RIPA buffer. Immunoprecipitates were fractionated by SDS-8% PAGE, followed by immunoblotting with anti-ubiquitin and/or rabbit polyclonal anti-ha antibodies.

RNAi-based Erk1/2 activation assay

For RNAi (siRNA)-based *Teb4* knockdown, HeLa cells (at ~70% confluence) in 6-well 35-mm plates were transfected with 100 pmol of *Teb4*-specific siRNA using Lipofectamin 2000 (Life technologies) for 24 hr. The cells were then co-transfected with 0.5 μg of M3 muscarinic acetylcholine receptor and 3 μg of either **MQ**-*Rgs2_ha* or control (pcDNA3.1(+)) plasmids per well in the serum-free Opti-MEM medium (Gibco). After 5 hr of transfection, the medium was replaced by DMEM containing 10% FBS. After incubation for 48 hr at 37°C, HeLa cells were subject to serum starvation in DMEM with 25 mM HEPES (pH 7.2) for 24 hr, followed by addition of M3 agonist carbachol (Sigma-Aldrich) for 10 min at the final concentration of 0.1 mM. Agonist-stimulated cells were washed twice in ice-cold phosphate-buffered saline (PBS) and thereafter lysed in RIPA buffer containing complete protease inhibitor cocktail (Roche) and phosphatase inhibitor mixture (Roche). Cells were then scraped into lysis buffer on ice and a lysate was clarified cell by centrifugation at 11,200g for 20 min at 4°C. Equal amounts of total protein in 1x SDS-sample buffer were heated at 95°C for 5 min, followed by SDS-10% Tris-glycine PAGE, and electrophoretic transfer onto PVDF membranes. The membranes were blocked for 1 hr at 4°C in PBS buffer containing 0.1% Tween 20 and 3% bovine serum albumin (Sigma-Aldrich), followed by immunoblotting with anti-phospho Erk1/2 or anti-Erk1/2 antibodies (Cell Signaling Technologies).

Chemical crosslinking and coimmunoprecipitation analyses

For crosslinking/coimmunoprecipitation assays, HeLa cell cultures (at ~75% confluence) in 10-cm dishes were co-transfected with 9 μg of pCH879 (expressing Teb4_f3) and 12 μg of either pCH766, or pCH822, or pcDNA3.1 (see above). After incubation for 24 hr, cells were treated with MG132 at 10 μM for 4 hr and thereafter with 1 mM Lomant's reagent (dithiobis(succinimidylpropionate (DSP)), a cell-penetrating amino group-specific crosslinking reagent. The *in vivo* crosslinking reaction was carried out on ice for 2 hr and was stopped by the addition of 10 mM Tris-HCl (pH 7.5) for 15 min at 25°C to quench unreacted DSP. Cells were gently scraped from plates, pelleted by low-speed centrifugation and lysed by resuspending them in 1 ml of buffer A (0.5% Triton X100, 0.15 M NaCl, 1 mM Na-EGTA, 0.1 mM $MgCl_2$, 10 mM HEPES, pH 7.4), plus *"complete protease inhibitor cocktail"* (Roche)) and incubating on ice for 20 min. The extracts were centrifuged at 11,200*g* for 20 min at 4°C and total protein concentrations in the supernatants were determined using Bradford assay (Bio-Rad). Samples containing 1 mg of total protein were incubated with anti-ha or anti-flag bound IgG Dynabeads (Life Technologies) at 4°C for 16 hr and the magnetic beads were washed 3 times in buffer A. Captured proteins were eluted in 15 μl of 0.1 M glycine-HCl (pH 2.8), followed by incubation in SDS-sample buffer containing 50 mM DTT for 30 min at 37°C, SDS-10% PAGE and immunoblotting with anti-ha or anti-flag as described above.

Purification of MQ-Rgs2$^{3-10}$-[GST] and GST-pulldown assays

To produce and purify the conditionally N^{α}-terminally acetylated (Nt-acetylated) **MQ**-Rgs2$^{3-10}$-[GST] fusion, we employed an *E.coli*-based expression system. "Wild-type" *E. coli* very rarely Nt-acetylates heterologous eukaryotic proteins. In the resulting novel system, **MQ**-Rgs2$^{3-10}$-[GST] was expressed in *E. coli* either by itself or together with the cognate (Nt-acetylating the Met-Gln N-terminal sequence) NatB Nt-acetylase complex from the fission yeast *Schizosaccharomyces pombe* (*32*). The plasmid pCH3080, expressing **MQ**-Rgs2$^{3-10}$-[GST], was transformed into *E. coli* BL21(DE3) that carried either a vector plasmid (pACYCDuet

(pCH15)) or pCH3025 (*32*), which expressed the *Naa20* and *Naa25* subunits of the *S. pombe* NatB Nt-acetylase in *E. coli*.

Overnight cultures (5 ml) of transformed *E. coli* were inoculated into LB medium (500 ml) containing chloramphenicol (34 μg/ml) and kanamycin (50 μg/ml), followed by growth at 37°C to A_{600} of ~0.7. Expression of **MQ**-Rgs2$^{3-10}$-[GST] was then induced with 1 mM isopropyl β-D-thiogalactoside (IPTG) at 30°C for 4 hr. Cells were harvested by centrifugation and frozen at -80°C. Cell pellets were thawed and resuspended in STE buffer (0.1 M NaCl, 1 mM Na-EDTA, 10 mM Tris-HCl, pH 8.0) containing 1 mM DTT, 1mM phenylmethylsulfonyl fluoride (PMSF) and 1 mg/ml of chicken egg white lysozyme (Sigma). Cell suspensions were incubated on ice for 20 min and thereafter treated by sonication for 1 min 3 times, at 1-min intervals, followed by the addition of Triton X100 to the final concentration of 1%. After centrifugation at 11,200g for 20 min at 4°C, the supernatants (~25 ml) were incubated with 1 ml of Glutathione Hicap agarose (50% slurry; Qiagen) at 4°C for 2 hr. The beads were washed twice in 25 ml of the STE buffer. Carrier-bound GST or **MQ**-Rgs2$^{3-10}$-[GST] were eluted with 1 ml of STE buffer containing 10 mM glutathione (GSH), followed by overnight dialysis against storage buffer (10% glycerol, 0.15 M NaCl, 10 mM β-mercaptoethanol, 50 mM HEPES, pH 7.5). The state of Nt-acetylation of the resulting **MQ**-Rgs2$^{3-10}$-[GST] fusion proteins was determined by MALD-TOF mass spectrometry.

For GST-pulldown assays, 50 μg of either GST, or **MQ**-Rgs2$^{3-10}$-[GST] (expressed in *E. coli* without *S. pombe* NatB), or (presumably) Nt-acetylated **MQ**-Rgs2$^{3-10}$-[GST] (coexpressed in *E. coli* with *S. pombe* NatB) were incubated with 50 μl of the Glutathione Hicap agarose beads in GST-loading buffer (10% glycerol, 0.5 M NaCl, 1% NP40, 1 mM Na-EDTA, 50 mM Tris-HCl, pH 8.0) at 4°C for 1 hr. The beads were washed once with 0.5 ml of the loading buffer and once with 0.5 ml GST-binding buffer (10% glycerol, 0.05% NP40, 50 mM NaCl, 50 mM Na-HEPES, pH 7.8). The beads in 0.2 ml-GST binding buffer were thereafter incubated at 4°C for 2 hr with 0.25 ml extracts from HeLa cell (2 mg of total protein) that expressed C-terminally triple flag-tagged (plus His$_6$-tagged) Teb4. The beads were washed 3 times in 0.5 ml of GST-binding buffer, followed by elution of bound proteins by the addition of 15 μl of 2xSDS-sample buffer and incubation for 30 min at 37°C. The resulting samples were fractionated by SDS-8% PAGE and analyzed by immunoblotting with anti-flag antibody. The blotting membrane was also stained with Coomassie Brilliant Blue to verify the approximate equality of total protein loads vis-à-vis GST, **MQ**-Rgs2$^{3-10}$-[GST] and Ac-**MQ**-Rgs2$^{3-10}$-[GST].

Analysis of endogenous MQ-Rgs2 from human cells by mass spectrometry

Purified human Rgs2 (~ 0.4 μg; see the first section of Materials and Methods) was treated with 8 M Urea in 25 mM NH$_4$HCO$_3$ (pH 8.0) and thereafter reduced with 9.5 mM DTT in 25 mM NH$_4$HCO$_3$ (pH 8.0) at 25°C for 1 hr. Rgs2 was then alkylated with iodoacetamide (32 mM) in NH$_4$HCO$_3$ (pH 8.0) at 25°C for 1 hr in the dark, followed by quenching of excess unreacted iodoacetamide with DTT (40 mM) at 25°C for 10 min. The sample was diluted 10-fold with 25 mM NH$_4$HCO$_3$ (pH 8.0), and 1 ml of the resulting sample was digested with of trypsin (1.2 μg/ml) overnight at 37°C. Nt-acetylated peptides in the digested sample were analyzed by nanoflow liquid chromatography-tandem mass spectrometry (LC-MS/MS) using the LTQ Orbitrap Velos (Thermo Scientific) hybrid mass spectrometer. Nt-acetylation sites were assigned by manual inspection of MS/MS spectra and also using MaxQuant software (*33*).